Atmospheric Environment 310 (2023) 119961

Contents lists available at ScienceDirect

Atmospheric Environment

journal homepage: www.elsevier.com/locate/atmosenv

Cloud condensation nuclei activation properties of Mediterranean pollen types considering organic chemical composition and surface tension effects

A. Casans [a,b,*], F. Rejano [a,b], J. Maldonado-Valderrama [b,c], J.A. Casquero-Vera [a,d,e], S. Ruiz-Peñuela [a,b], B.L. van Drooge [e], H. Lyamani [a,f], A. Cazorla [a,b], E. Andrews [g,h], Jack J. Lin [i], F. Mirza-Montoro [j], D. Pérez-Ramírez [a,b], F.J. Olmo [a,b], L. Alados-Arboledas [a,b], P. Cariñanos [a,k], G. Titos [a,b]

[a] Andalusian Institute for Earth System Research IISTA, University of Granada, 18006, Granada, Spain
[b] Department of Applied Physics, University of Granada, 18071, Granada, Spain
[c] Unidad de Excelencia Internacional "Modeling Nature" (MNat), University of Granada, Spain
[d] Institute for Atmospheric and Earth System Research (INAR)/Physics, Faculty of Science, University of Helsinki, Helsinki, Finland
[e] Institute of Environmental Assessment and Water Research (IDAEA), CSIC, 08034, Barcelona, Spain
[f] Department of Applied Physics, University of Málaga, 29010, Málaga, Spain
[g] Cooperative Institute for Research in Environmental Sciences, University of Colorado, Boulder, CO, 80309, United States
[h] Global Monitoring Laboratory, NOAA, Boulder, CO, 80305, United States
[i] Center for Atmospheric Research, University of Oulu, P.O. Box 4500, 90014, Oulu, Finland
[j] Institute of Geophysics, Faculty of Physics, University of Warsaw, 00-927, Warsaw, Poland
[k] Department of Botany, University of Granada, 18071, Granada, Spain

HIGHLIGHTS

- Subpollen particles (SPPs) show κ values in the 0.1–0.3 range.
- SPPs activate as CCN at atmospheric supersaturation conditions.
- Saccharides and fatty acids are organic compounds found in all pollen types.
- The droplet surface tension reduction is observed at high concentration of SPPs.
- Reduction of surface tension does not show a relevant effect on SPP activation.

GRAPHICAL ABSTRACT

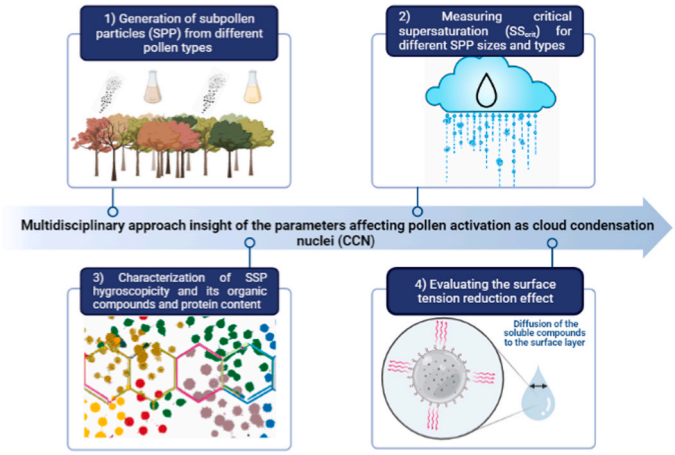

* Corresponding author. Andalusian Institute for Earth System Research IISTA, University of Granada, 18006, Granada, Spain.
E-mail address: andreacasans@ugr.es (A. Casans).

https://doi.org/10.1016/j.atmosenv.2023.119961
Received 15 March 2023; Received in revised form 13 July 2023; Accepted 14 July 2023
Available online 15 July 2023

ARTICLE INFO

Keywords:
Aerosol
Pollen
Cloud condensation nuclei
Hygroscopicity
Surface tension

ABSTRACT

Wind-dispersed pollen grains emitted from vegetation are directly injected into the atmosphere being an important source of natural aerosols globally. These coarse particles of pollen can rupture into smaller particles, known as subpollen particles (SPPs), that may act as cloud condensation nuclei (CCN) and affect the climate. In this study, we characterize and investigate the ability of SPPs of 10 Mediterranean-climate pollen types to activate as CCN. A continuous flow CCN counter (CCNC) was used to measure the activation of size-selected (80, 100 and 200 nm dry mobility diameter) particles at different supersaturations (*SS*). Hygroscopicity parameter (κ) for each SPP type and size has been calculated using κ-Köhler theory. Organic chemical speciation and protein content has been determined to further characterize pollen solutions. Furthermore, the surface activity of SPPs has also been investigated by using pendant drop tensiometry. All studied SPP samples show critical supersaturation (SS_{Crit}) values that are atmospherically relevant *SS* conditions. Hygroscopicity κ values are in the range characteristic of organic compounds (0.1–0.3). We found that organic speciation and protein content vary substantially among pollen types, with saccharides and fatty acids being the only organic compounds found in all pollen types. A clear relationship between SPP activation and its organic composition was not observed. This study also reveals that all SPPs investigated reduce the surface tension of water at high concentrations but at diluted concentrations (such as those of activation in the CCNC), the water surface tension value is a good approximation in Köhler theory. Overall, this analysis points out that pollen particles might be an important source of CCN in the atmosphere and should be considered in aerosol-cloud interactions processes.

1. Introduction

Atmospheric aerosol particles play an important role in physical and chemical processes that occur in the atmosphere, causing a significant impact on Earth's energy balance (e.g., Andreae and Rosenfeld, 2008; Rama et al., 2022; Zieger et al., 2013) through direct and indirect effects. Direct effects are related to scattering and absorption of solar radiation by particles while indirect effects result from changes in cloud droplet properties due to activation of aerosols as cloud condensation nuclei (CCN) and ice nuclei (IN) (e.g., Seinfeld et al., 1998; Andreae and Rosenfeld, 2008; Fröhlich-Nowoisky et al., 2016; Burkart et al., 2021; Rejano et al., 2021).

Atmospheric particles can be directly emitted into the atmosphere from natural or anthropogenic sources (primary particles), or can be formed in the atmosphere from precursor vapours (secondary particles) (e.g., Kanakidou et al., 2005). Among primary aerosol particles, increased attention has recently been paid to primary biological aerosol particles (PBAPs) due to their impact on human health and aerosol-climate interactions (Deguillaume et al., 2008; Després et al., 2012; Rose et al., 2010; Tanarhte et al., 2018). PBAPs include bacteria, fungi, spores, decayed organic matter, plants fragments, viruses, algae or pollen (Fröhlich-Nowoisky et al., 2016; Pope, 2010). Laboratory experiments have demonstrated that several types of PBAPs (such as pollen, spores and bacteria) can act as CCN and IN at atmospherically relevant conditions (Burkart et al., 2021; Hoose and Möhler, 2012; Mikhailov et al., 2019; Pöschl et al., 2010; Pummer et al., 2012; Steiner et al., 2015).

Among PBAPs, pollen emissions from vegetation are an important source of aerosol particles globally (Andreae and Rosenfeld, 2008; Després et al., 2012; Pöschl et al., 2010), with an emission rate into the atmosphere currently estimated at 47 Tg/year (Hoose et al., 2010). This emission rate is expected to increase in the future due to climate change (Zhang and Steiner, 2022). Pollen particles tend to have a short lifetime in the atmosphere due to their large size, ranging from 10 to 100 μm (Després et al., 2012; Manninen et al., 2014). However, recent studies have shown that under high humidity conditions, as well as a consequence of mechanical impacts, pollen grains can rupture into smaller particles (from several nanometers to 1 μm) called subpollen particles (SPPs) (Després et al., 2012; Grote et al., 2003; Mikhailov et al., 2019; Taylor et al., 2004). Some estimates suggest that one pollen grain can form up to thousands of SPPs (Hughes et al., 2020; Stone et al., 2021). This leads to increased residence time in the atmosphere and may enhance the direct and indirect influence of pollen on climate. Recent studies have shown that these SPPs can potentially affect climate via aerosol-cloud interaction by acting as CCN (Mikhailov et al., 2019, 2021; Prisle et al., 2019; Steiner et al., 2015).

The ability of aerosol particles to activate as CCN depends on their size, chemical composition, water solubility, hygroscopicity (κ) and morphology (Bougiatioti et al., 2017; Dusek et al., 2006; Ervens et al., 2010; Petters and Kreidenweis, 2008). Activation and hygroscopic properties of inorganic particles are well defined in the literature (Sorjamaa et al., 2004). However, these characteristics are still poorly understood for organic aerosols (OA) and especially for aerosol organic mixtures (such as SPPs) (Prisle et al., 2019). Pollen particles contain many organic biomolecules (Pacini et al., 2006), like fatty acids (Ischebeck, 2016), amino acids (Gong et al., 2015; Lawson et al., 2021), proteins (Steiner et al., 2015) and saccharides (Mampage et al., 2022; Pacini et al., 2006; Rathnayake et al., 2017). However, the relative contribution of the different compounds in pollen varies among species (Axelrod et al., 2021) which might influence their activation and hygroscopic properties. These compounds have different water solubility properties which could also impact CCN activity. Results on the link between specific chemical constituents in SPPs and their activation ability or hygroscopicity are inconclusive (Mikhailov et al., 2021; Steiner et al., 2015).

In addition, some of these constituents can act as surfactants capable of reducing surface tension. The importance of surface tension reduction (and its time evolution) on SPPs activation as CCN, has previously been studied, however, it is still not well understood (e.g. Davies et al., 2019; Forestieri et al., 2018; Lin et al., 2020; Petters and Kreidenweis, 2013; Sorjamaa et al., 2004; Varga et al., 2007). This is because the presence of surfactants can have opposing effects on aerosol activation related to Kelvin and Raoult effects (described in Köhler Theory) (Köhler, 1936). Surfactants reduce the surface tension, decreasing critical supersaturation and facilitating particle activation (Kelvin effect). In contrast, the depletion of solute from the droplet bulk (surfactant partitioning effect), in which the surfactant migrates to the surface, might reduce the hygroscopic water uptake and therefore, reduce the activation efficiency (Raoult effect). It is an active area of research to determine whether the reduction of surface tension prevails over solute effect increasing activation efficiency (e.g., Ovadnevaite et al., 2017) or if, in contrast, the surface partitioning effect is dominant, which limits the activation of particles (Sorjamaa et al., 2004; Forestieri et al., 2018). Thus, further studies are needed to explain these discrepancies and improve our understanding in this topic.

In this study, we investigate the CCN activation ability of different SPP types, representatives of the Mediterranean basin, through different laboratory experiments to better understand the influence of organic chemical compounds, their solubility and surface tension effects in activation properties and hygroscopicity of SPPs. Additionally, we have

studied surface activity of SPPs, to determine if it should be considered in Köhler theory. The combined discussion of different experimental variables offers new information which can be of great interest to better understand the potential atmospheric and climate impact of SPPs.

2. Methodology

In this section we describe the methodology followed to perform a comprehensive analysis of subpollen particles activation as CCN, from pollen recollection and sample preparation to SPP generation and laboratory studies including CCN activation, surface tension, and chemical and protein content determination.

2.1. Pollen sampling and SPP generation

Fresh pollen samples of common plant species characteristic of Mediterranean climate have been collected directly from trees in the Granada area (37.18°N, 3.58°W, 680 m a.s.l., Spain) during the flowering season in 2021 (Cariñanos et al., 2022). The plant species collected for this study were: *Cupressus sempervirens, Dactilys glomerata, Olea europeae, Pinus* spp., *Platanus hispanica, Acer negundo, Fraxinus angustifolia, Populus nigra* and *Quercus rotundifolia*. Additionally, we have analysed pollen samples from *Olea europeae* collected in 2019 flowering season and commercial samples of *Populus* (tree pollen *Populus deltoides,* Reference product P7395-1G, Merck). All these species are linked to plant communities characteristic of the Mediterranean region: different species of *Pinus* and *Quercus* form the main natural sclerophyllous forest formations (Vilà et al., 2007); *Olea* has the largest cultivated area in the Mediterranean region (more than 90%) (Guerrero et al., 2016; Fraga et al., 2021), while *Cupressus*, *Platanus*, *Acer, Fraxinus* and *Populus* are present in natural communities, cultivated, and integrated into the urban forests of the cities in the region (Krajter Ostoić et al., 2018; Cariñanos et al., 2020). Grasses (which include *Dactylis glomerata*) are one of the largest botanical families with representation in practically all terrestrial biomes, including the Mediterranean scrub (Molina et al., 2023).

After collection, samples were stored for two days at room temperature to dry them out. Later, they were sifted to separate pollen from flowers and spurious particles. Finally, each pollen sample was stored in a refrigerator at 3 °C. Organic pollen dispersions were prepared by adding 0.5 g of pollen to 300 mL of ultrapure water (Milli-Q, 0.054 μS) and shaking mechanically for 15 s to allow pollen grains to break into subpollen particles (Steiner et al., 2015). Rupture of pollen grains was confirmed by Scanning Electron Microscopy (SEM; ZEISS operating at 5 kV accelerating voltage and 2.9 mm working distance). SPP dispersions were left in the refrigerator at 3 °C for 1 h and then filtered three consecutive times using 47 mm diameter quartz microfibers filters with 0.45 μm pore size (Pall Corporation, New York, USA) to remove any large pollen particles. These solutions were then used for the following described experiments.

2.2. Cloud condensation activity of size-selected SPP

The filtered solutions were aerosolized using an Aerosol Generator (TSI 3076) and passed through a diffusion dryer connected to a small dilution chamber to stabilize the generated particle number concentrations. The resulting particles entered a Scanning Mobility Particle Sizer (SMPS, TSI 3938), where particles were charged by a neutralizer (TSI 3088) prior to the Differential Mobility Analyzer (DMA, TSI 3081A) where particles of different sizes were selected. In this study, subpollen particles with electric mobility diameters size of 80, 100 and 200 nm were selected. To ensure the size-selection, the DMA was calibrated at the beginning and the end of the experiments by using 203 nm polystyrene latex particles (PSL). Once particles of a certain size were selected by the DMA, the monodisperse aerosol flow was split between: 1) a Condensation Particle Counter (CPC, TSI 3372) to provide the particle number concentration (N_{CN}) for each selected size (a concentration of around 2000-4000 particles cm^{-3} was maintained) and 2) a Continuous-Flow Streamwise Thermal Gradient Cloud Condensation Nuclei Counter (CCNC, DMT model CCN-100) to provide the number of particles that are activated (N_{CCN}) for each selected size.

The design of the CCNC is based on a cylindrical continuous-flow thermal-gradient diffusion chamber where constant temperature gradients are applied, generating different supersaturation conditions and maximizing the growth rate of activated particles (Roberts and Nenes, 2005). The instrument was calibrated at the beginning and at the end of the experiments, using ammonium sulphate and following ACTRIS guidelines (available in http://actris.nilu.no/Content/SOP). The CCNC operated at 0.5 lpm flow rate with a sheath-to-aerosol flow ratio of 10. The water vapour supersaturation (*SS*) was regulated by the temperature gradient inside the CCNC column. For each selected diameter (80, 100 and 200 nm), the *SS* was scanned over 10 different *SS* values (Table 1 shows the *SS* used for each particle size), taking 5 min at each *SS*. It should be mentioned that the DMT CCNC exhibits kinetic limitations under low *SS* conditions (<0.1%) that could affect CCN measurements leading to increased uncertainties in SS_{Crit} estimations at low *SS* (Lance et al., 2006; Wang et al., 2019; Yang et al., 2012). The accuracy in supersaturation is ±10% (relative) when *SS* are higher than 0.2% and ±0.03% (absolute) when *SS* are lower than 0.2% (http://actris.nilu.no/Content/SOP). Despite the larger uncertainties and limitations at *SS*<0.1%, the *SS* table for 200 nm particles includes *SS* values below this limit. This was necessary to determine the SS_{Crit} for large SPPs that was expected to be between 0.05 and 0.12%. A detailed analysis and discussion of associated uncertainties is presented in Section 3.1.

The measurements obtained were interpreted using κ-Köhler theory which included a simplification of the Raoult term in the Köhler equation (Köhler, 1936). The hygroscopicity parameter, κ, ranges from 0 (insoluble or non-hygroscopic substances) to 1.4 (very soluble or hygroscopic substances such as sodium chloride). The κ-Köhler model expresses the equilibrium curve of the saturation ratio, *S*, over an aqueous solution drop with diameter, *D*:

$$S(D) = \frac{D^3 - D_{dry}^3}{D^3 - D_{dry}^3(1-\kappa)} exp\left(\frac{4\sigma M_w}{RT\rho_w D}\right) \quad (1)$$

where ρ_w and M_w are the density and molecular weight of water, respectively; *R* is the universal gas constant, *T* is the absolute temperature and σ is the droplet surface tension (assumed to be equal to the surface tension of pure water, 72 mN/m). Eq. (1) can be expressed in terms of the supersaturation (*SS*), which is commonly defined as $(S - 1) \bullet 100$. The maximum of the Köhler curve, *SS (D)*, is called critical supersaturation (SS_{Crit}), and establishes the activation threshold for a particle with diameter *D*.

To obtain the SS_{Crit} it is necessary to know the activation fraction (*AF*), defined as N_{CCN}/N_{CN}, for different *SS* values. The obtained activation spectra at each size is normalized to the maximum observed for each pollen type (Steiner et al., 2015) and fitted to a cumulative Gaussian distribution as function of supersaturation (Mei et al., 2013; Rose et al., 2008; Thalman et al., 2017).

$$AF = a\left(1 + erf\left(\frac{SS - SS_{Crit}}{\beta\sqrt{2}}\right)\right) \quad (2)$$

where *a* is half the maximum value of *AF* (ideally 0.5), *erf* is the error function, β is the standard deviation of the cumulative Gaussian distribution and SS_{Crit} is the value of supersaturation when *AF* is 0.5. We can retrieve experimental values of SS_{Crit} by fitting *AF* and *SS* data to Eq. (2). The hygroscopicity parameter for each pollen type was determined following a similar methodology as Rose et al. (2010) and Prisle et al. (2019). Specifically, in Eq. (1), κ values were varied from 0 to 0.5 and *D* values were varied in the range D_{dry} to 2000 nm. κ is the value that minimizes the difference between SS_{Crit} derived from Eq. (1) and

Table 1
SS values selected to study the activation for SPPs of 200, 100 and 80 nm.

Size (nm)	*SS* (%)									
200	0.01	0.02	0.04	0.06	0.08	0.1	0.2	0.4	0.6	0.8
100	0.1	0.15	0.2	0.22	0.25	0.28	0.3	0.4	0.6	0.8
80	0.1	0.15	0.2	0.24	0.28	0.3	0.34	0.38	0.5	0.8

experimental SS_{Crit} from Eq. (2).

2.3. Surface tension measurements

The surface tension of filtered pollen solutions was measured using a Pendant Drop Tensiometer developed at the University of Granada (Cabrerizo-Vílchez et al., 1999). Sample preparation was performed following the procedure explained in Sect. 2.1. Due to variation in filtration efficiency of the different pollen types, the actual concentration in the solutions differs among pollen species. These concentrations were calculated by placing 100 μL of the solutions on aluminium foil surfaces, evaporating the water in a furnace (at 60 °C for 1 h) and weighing the resulting sample. The initial concentrations of *Populus deltoides, Populus nigra*, *Quercus*, *Dactilys* and *Fraxinus* were 5 g/L and the initial concentration of *Pinus* was 50 g/L. These solutions were then diluted 10, 100 and 1000 times in ultrapure water. To ensure that there were no contaminant substances, the surface tension of pure water (σ_w) was measured between each pollen solution yielding the expected value of 72.5 ± 1.5 mN/m at room temperature (23 °C) (Maldonado--Valderrama et al., 2004).

Once solutions were prepared, the experimental setup was used to measure surface tension. The technique consists in acquiring the silhouette of an axisymmetric fluid droplet and iterative fitting over the Young-Laplace equation which represents the balance between gravitational deformation of the drop and the surface tension (Berry et al., 2015). The shape of the pendant drop exhibits a curvature that depends on the competition between gravity and interfacial tension. This curvature can be described theoretically by the Young-Laplace equation of capillarity:

$$\sigma\left(\frac{1}{R_1}+\frac{1}{R_2}\right)=\Delta P=\Delta P_0-\Delta\rho g z \tag{3}$$

where R_1 and R_2 are the central radii of curvature, $\boldsymbol{\sigma}$ is the surface tension of the droplet solution, ΔP_0 is the reference pressure at z = 0 (drop apex), $\Delta\rho$ is the density difference between both fluids (droplet and air), g is the gravity acceleration, and z is the vertical coordinate.

Very briefly, the system is based on a CCD (Charge-Coupled Device) video camera (Pixelink), connected to an optical microscope (Edmund Optics), a diffused light source to avoid aberrations and spurious reflections and a microinjector (Hamilton PSD3 Half-Height Syringe Pump) connected to a Teflon capillary where the pendant drop of solution is formed. A schematic of the experimental setup is shown in Maldonado-Valderrama et al. (2021). The equipment sits on a vibration isolation table 'Kinetic System Inc. Vibraplane' to prevent vibration during the experiments. The video camera takes multiple images of the pendant drop at different instants in time, capturing the variations of the droplet shape as the surface tension changes.

The whole experimental setup is computer controlled by software DINATEN© (University of Granada) which processes the digitized images of pendant drops and extracts the experimental drop profiles, which are fitted later to the Young-Laplace equation of capillarity (Eq. (3)) by using Axisymmetric Drop Shape Analysis (Hoorfar and Neumann, 2006). The program provides as outputs, the drop volume (V), the surface tension (σ), and the interfacial area (A). The pendant drop with the aqueous solution (20 μL) is formed at the end of the capillary. The measurement process is registered at a constant surface area (32 mm^2) (Cabrerizo-Vílchez et al., 1999).

2.4. Organic compounds identification

Pollen from different plant species were analysed for their saccharide and organic acid content. Twenty five μL of surrogate standards levoglucosan-d7 (Cambridge Isotopic Laboratories, UK) and succinic acid-d4 (Sigma Aldrich) were added to a vial (Merck, Darmstadt, Germany) to which between 0.1 and 20 mg of pollen in 0.5 mL of methanol was added (Medeiros and Simoneit, 2007). Extraction was done in an ultrasonic bath for 15 min.

After extraction, the sample was transferred to a vial and evaporated to dryness under a N_2-gas stream. Then, 25 μL of bis (trimethylsilyl) trifluoroacetamide (BSFTA)+trimethylchlorosilane (99 : 1) (Supelco) and 10 μL of pyridine (Merck) were added for derivatization of the polar compounds to their trimethylsilyl esters at 70 °C during 1 h. Before analysis, 100 μL of isooctane was added to the vial. Sample extracts were injected into a gas chromatograph coupled to a mass spectrometer (Thermo Trace GC Ultra – DSQ II) equipped with a 60 m fused capillary column (HP-5MS 0.25 mm × 25 μm film thickness). The oven temperature program started at 60 °C held for 1 min, and then heated at 12 °C/min to 120 °C and to 320 °C at 4 °C/min, where it was held for 15 min. The temperatures of the injector, ion source, quadrupole and transfer line were 280 °C, 200 °C, 150 °C and 280 °C, respectively. Helium was used as a carrier gas at 0.9 mL/s. The MS selective detector was operated in full scan (m/z 50–650) and electron impact (70 eV) ionization modes. Compounds were identified with authentic standards and the corresponding retention times in the chromatograms (Fontal et al., 2015). The recoveries of the surrogate standards were higher than 70% in all samples. Analytical blank levels were lower than 1% of the sample levels. Limits of quantification (LOQ) were calculated by dividing the lowest measured levels in the standard calibration curves by the mass of the analysed sample fraction. These were 0.4 ng/mg for the saccharides and 0.06 ng/mg for the acids.

2.4.1. Protein content

The protein content of the different pollen samples was analysed at Research Support Central Service of the University of Córdoba (Spain). Each pollen type was dissolved as explained in Sect. 2.1 with the same concentration, matching that used to generate SPPs. Protein content in the solutions was determined using the "Bradford assay" method (Bradford, 1976). It consists of a protein quantification technique based on variation in absorbance produced by the colour change of Coomassie Brilliant Blue G-250 (Bio-Rad Protein Assay). The maximum absorbance of the dye changes from 465 nm to 595 nm, when it is linked to the protein. The absorbance at 595 nm is directly proportional to the protein concentration in the sample. Therefore, the calibration curve was obtained using Bradford reactive (Bio-Rad Protein Assay Dye Reagent concentrate, 450 mL, #5000006) and known concentrations of a standard protein. Then, the protein content in each sample was determined by measuring the absorbance of each solution at 595 nm using this calibration curve.

3. Results and discussion

In this section, we first show the activation properties (critical supersaturation and hygroscopicity parameter) of SPPs of 11 pollen samples (10 pollen types) of different dry sizes. Because chemical composition and surface tension have an impact on the observed CCN activation, Section 3.2. presents the organic composition and protein

content of each pollen type and Section 3.3. describes the surface activity of some of the pollen types analysed.

3.1. Activation properties: critical supersaturation and hygroscopicity

Fig. 1 shows the measured CCN activity (i.e., critical supersaturations) of SPPs of 11 pollen samples of different dry size (80, 100 and 200 nm diameter) together with the calibration points with ammonium sulphate and the theoretical range of SS_{Crit} for ammonium sulphate as a reference for hygroscopic particles according to Gysel et al. (2002) and Topping et al. (2005). All SPPs studied exhibited similar activation abilities, with slight differences among different species. The SS_{Crit} values obtained for all pollen types correspond to supersaturations values that can be found in the atmosphere, which evidences that the SPPs analysed here can act as cloud condensation nuclei at atmospherically relevant conditions.

The obtained SS_{Crit} range between (0.07–0.12) %, (0.17–0.28) % and (0.25–0.37) % for 200 nm, 100 nm and 80 nm particle diameters, respectively (Fig. 1). SS_{Crit} uncertainties have been calculated as the standard deviation of the SS_{Crit} values obtained by varying the measured SS within its range of uncertainty (±10% relative for SS>0.2% and ±0.03% absolute for SS<0.2%) (Schmale et al., 2017). SS_{Crit} values obtained in this study are in the lower range of previously reported values by Steiner et al. (2015) and Mikhailov et al. (2019). The studies mentioned before investigated a lower number of pollen types, while here we explore the activation ability of 10 different species characteristics of the Mediterranean area. Our results show that SS_{Crit} values depend mainly on the SPP size, however, differences are observed among species for each size indicating different CCN activity for each pollen type. *Quercus* is the pollen type with the highest SS_{Crit} values for all sizes, denoting its lower activation ability. The highest activation ability is found for those pollen types with the lowest SS_{Crit}: *Populus nigra* for 80 nm, *Populus deltoides* for 100 nm and *Cupressus* for 200 nm.

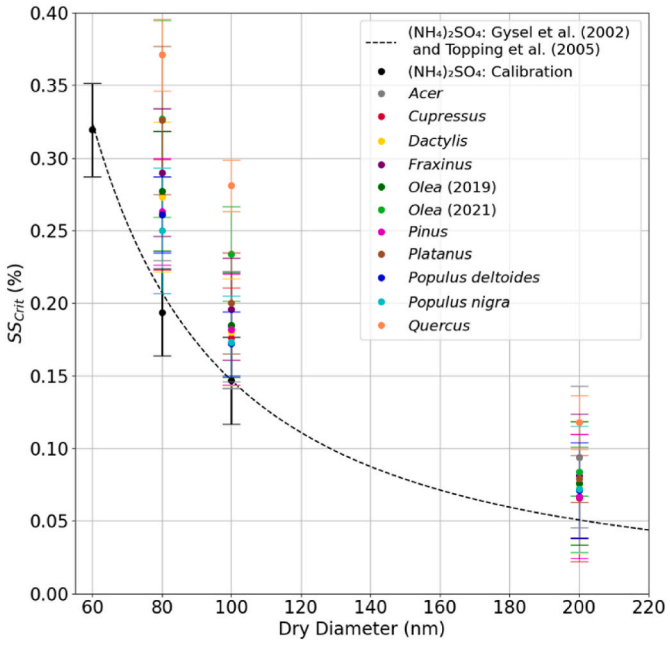

Fig. 1. *Critical supersaturations (SS_{Crit}) of the 11 analysed pollen samples at different dry diameters (80, 100 and* 200 nm*). Error bars for each pollen type correspond to the standard deviation of SS_{Crit} calculated considering the uncertainties in measured SS (see the text for further detail in uncertainty calculation). Black line represents the theoretical range of SS_{Crit}* for ammonium sulphate *($(NH_4)_2SO_4$)* (Gysel et al., 2002; Topping et al., 2005)*, black points are SS_{Crit} values of $(NH_4)_2SO_4$ obtained during CCNC calibration at 60, 80 and* 100 nm *and their respective error bars that have been calculated considering SS uncertainties (± 10% for* 60 nm *and ± 0.03% absolute SS for 80 and* 100 nm*).*

Fig. 1 also shows that the two *Olea* pollen specimens investigated exhibit different activation behaviours, especially at 100 nm (SS_{Crit} values are 0.23% for *Olea*, 2021 and 0.19% in *Olea* 2019) and 80 nm (0.33%, *Olea* 2021 and 0.28%, *Olea* 2019). This could indicate that *Olea* collected in 2019 might have experienced some chemical degradation, in some of its organic components, over time affecting its CCN activity. On the other hand, *Populus nigra* and *Populus deltoides* have almost indistinguishable SS_{Crit} values for all sizes. SS_{Crit} values for *Populus nigra* (non-commercial) are 0.25%, 0.17% and 0.07% for 80, 100 and 200 nm, respectively. *Populus deltoides* (commercial) yields SS_{Crit} values at 80, 100 and 200 nm of 0.26%, 0.17% and 0.07%. *Populus deltoides* properties might differ from natural ambient pollens due to the commercial sample preparation, however, the analogous SS_{Crit} values obtained for both indicate that using commercial pollen types to investigate CCN activation properties provides similar results as the natural samples, at least for these species.

As we have mentioned above, the CCNC exhibits kinetic limitations related to droplet growth. In the CCNC measurements, the CCN identification criteria is based on a threshold diameter (0.75 μm) from which all particles are considered activated (https://dropletmeasure.wpengineepowered.com/wp-content/uploads/2020/02/DOC-0086-Rev-N-CCN-Manual.pdf). However, unactivated particles may also grow to such a diameter due to hygroscopic growth. Using this default cut off diameter can lead to 30% overestimation of the bulk CCN number concentration measurements for SS lower than 0.1% (Yang et al., 2012; Tao et al., 2023). Furthermore, there are higher uncertainties in the CCNC column temperature gradient at low SS (<0.05%). The accuracy in supersaturation is ±10% (relative) when SS are higher than 0.2% and $\Delta SS \leq 0.03\%$ (absolute) when SS are lower than this value (http://actris.nilu.no/Content/SOP). It is important to bear in mind these shortcomings of the CCNC at low SS in our study since the calculated SS_{Crit} values for 200 nm particles are within the range 0.07–0.12%. In addition, SS<0.05% have been used to determine those SS_{Crit} values (see SS table, Table 1). To check for deviations in the estimated SS_{Crit} for 200 nm SPPs particles due to potential CCNC overcounting issues, we have re-calculated the SS_{Crit} assuming an overestimation of 30% at SS<0.1% and determined that the SS_{Crit} values were within the estimated uncertainty. This 30% overestimation is expected to be lower for organic particles (Yang et al., 2012; Ruehl et al., 2008; Shantz et al., 2012), such as SPPs. Therefore, the SS_{Crit} values reported in this study are not substantially affected by CCNC limitations at low SS, and the associated uncertainties have been estimated so they take into account the lower accuracy of the instrument at low SS. Further studies investigating how to correct for kinetic limitations are required to improve CCN activation properties accuracy at low SS.

To describe the SPP hygroscopicity, κ values have been calculated for each pollen type at each size using Eq. 1 and the results are given in Table 2. All pollen types show similar κ values with size (except *Acer*), indicating that κ is mostly independent from the particle size. Prisle et al. (2019) and Mikhailov et al. (2021) also found a weak dependency of κ with size. The differences observed here are in the range 0–20% for all pollen types, except *Acer*, which shows differences higher than 50% (53.6%). This could be due to unstable and higher SPP concentration at 200 nm during the experiments with *Acer*. As explained in Sect. 2.2, total concentration of particles was kept in the range 2000–4000 particles/cm^3. However, during the experiments with *Acer* at 200 nm, concentrations were unstable. Therefore, the average κ values (considering all pollen types, except *Acer* at 200 nm) for 80, 100 and 200 nm SPPs are 0.29, 0.29 and 0.28, respectively. Hygroscopicity κ values are within the range 0.137 ± 0.018 (*Quercus*) and 0.328 ± 0.019 (*Cupressus*), characteristic of moderately hygroscopic organic aerosols (Petters and Kreidenweis, 2007). Previous studies showed that organic aerosol particles exhibit a wide range of κ values ranging from 0 to 0.3 (e.g., Dusek et al., 2010; Pöhlker et al., 2016; Thalman et al., 2017). In this work, the κ for most pollen types is approximately 0.3, suggesting pollen could be

Table 2
Mean hygroscopicity parameter, κ, obtained for each pollen type at 200, 100 and 80 nm dry diameter. Acer concentration at 200 nm was unstable. Therefore, its κ value is not considered in κ mean results.

Pollen Types	Dry Diameter (nm)			*κ (mean)*
	200	100	80	
Acer	0.17 ± 0.03	0.30 ± 0.10	0.27 ± 0.08	0.287 ± 0.022
Cupressus	0.34 ± 0.05	0.31 ± 0.06	0.34 ± 0.06	0.328 ± 0.019
Dactylis	0.30 ± 0.03	0.31 ± 0.06	0.31 ± 0.05	0.307 ± 0.005
Fraxinus	0.256 ± 0.014	0.30 ± 0.05	0.28 ± 0.04	0.280 ± 0.023
Olea 2019	0.28 ± 0.03	0.32 ± 0.06	0.30 ± 0.05	0.301 ± 0.017
Olea 2021	0.236 ± 0.011	0.236 ± 0.019	0.243 ± 0.015	0.238 ± 0.004
Pinus	0.33 ± 0.04	0.32 ± 0.06	0.32 ± 0.07	0.325 ± 0.010
Platanus	0.266 ± 0.019	0.29 ± 0.05	0.239 ± 0.015	0.28 ± 0.03
Populus nigra (non-commercial)	0.31 ± 0.04	0.30 ± 0.06	0.32 ± 0.05	0.311 ± 0.012
Populus deltoides (commercial)	0.32 ± 0.04	0.31 ± 0.06	0.33 ± 0.06	0.321 ± 0.015
Quercus	0.117 ± 0.008	0.146 ± 0.024	0.150 ± 0.022	0.137 ± 0.018
κ (mean) for all pollen types	0.28 ± 0.07	0.29 ± 0.05	0.29 ± 0.06	0.283 ± 0.006

considered a good surrogate for more hygroscopic organic species (Ruehl et al., 2016).

It should be noted that *Quercus* is the least hygroscopic species (Fig. 1 and Table 2) exhibiting the highest SS_{Crit}.. κ values are arranged from 0.11 to 0.15 and they are very similar to the SPP κ values obtained by Thalman et al. (2017), Mikhailov et al. (2019, 2021) and Prisle et al. (2019). The differences found between fresh *Olea* (2021) ($\kappa \sim 0.24$) and *Olea* (2019) ($\kappa \sim 0.30$) should also be highlighted. This could be due to aging of *Olea* collected in 2019, leading to an increase in κ.

3.2. Organic composition

Hygroscopic properties of inorganic compounds are well defined, however large uncertainties are associated with the effect of organic compounds on cloud droplet activation (Dawson et al., 2020; Sorjamaa et al., 2004). Previous studies have demonstrated the negative relationship between aerosol hygroscopicity at sub-saturated conditions and organic content (Burgos et al., 2020; Chen et al., 2018; Quinn et al., 2005; Titos et al., 2014), but the role of different organic components is still unclear especially in complex organic aerosol mixtures (Axelrod et al., 2021; Petters and Petters, 2016). In this section, we explore the relationship between organic concentration, organic speciation, protein content and aerosol hygroscopicity (κ parameter calculated at super-saturated conditions).

Fig. 2 shows the total concentration of organic compounds and protein content for each pollen type and the κ values (results of organics concentration for *Platanus* are not shown due to unavailability of this pollen type for GC-MS analysis). The protein and organic contents are highly variable among pollen types. *Pinus* and *Olea* 2021 are the pollen types with the highest concentration of organics (*Olea* 2021 has 90800 ng/mg and *Pinus* 88000 ng/mg). However, other species (*Acer*, *Populus deltoides* and *Quercus*) are the pollens with the highest protein content. The lowest organic concentrations are found for *Olea* 2019 (6000 ng/mg), *Cupressus* (4416 ng/mg) and *Acer* (4411 ng/mg). *Dactylis*, *Fraxinus*, and *Populus deltoides* have organic concentrations ranging from 36600 ng/mg to 44100 ng/mg; and finally, *Quercus* and *Populus nigra* have an organic content of 13400 ng/mg and 20700 ng/mg, respectively. *Cupressus* has the lowest proteins concentration (0.41 mg/mL) and the rest of pollen types show values in the range 1.10–1.60 mg/mL. Two things should be highlighted: (1) *Populus deltoides* has higher concentrations of organics and proteins than *Populus nigra* and (2) the composition of *Olea* 2019 and *Olea* 2021 is quite different which may explain differences in SS_{Crit} and κ for the two samples.

Regarding the hygroscopicity parameter, there is no significant relationship with the organics or proteins content. *Quercus* has the lowest κ value and the lowest organic concentration, but the highest protein content. *Acer* shows similar organic and protein content to *Quercus*, but it exhibits a higher κ value. Steiner et al. (2015) pointed out that the protein content might play a role in determining SPP hygroscopicity. These authors observed that, from the 6 pollen types they investigated, *Ambrosia* (not studied here) showed the highest SS_{Crit} and the highest protein content; but they also did not find a clear trend with κ. Similarly, Mikaihlov et al. (2021) did not observe a direct relationship between organic concentration and pollen hygroscopicity.

To relate SPP hygroscopicity to its organic content, we have to take into account that organic compounds cover hundreds of different

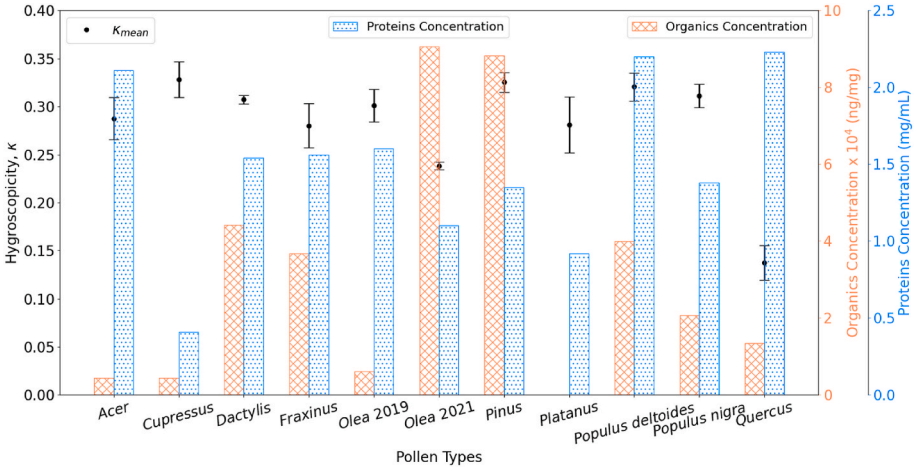

Fig. 2. Bar diagram showing total organic compound concentration (in ng/mg of pollen), protein content (in mg/mL) and mean hygroscopicity parameter κ for each pollen type. The κ error bars represent the standard deviation for the three dry size diameters investigated.

chemical components (Oros and Simoneit, 2001; Rissanen et al., 2006) that can exist in the atmosphere affecting the ability of aerosol particles to act as CCN (Raymond and Pandis, 2002). Studies investigating the ability of individual organic components (such as oleic acid, stearic acid, levoglucosan, glucose, glutamic acid or palmitic acid) have clearly shown their different hygroscopic and activation properties (Abbatt et al., 2005; Dawson et al., 2020; Kristensson et al., 2010; Nguyen et al., 2017; Rosenørn et al., 2006) and many of these organic compounds have been identified in pollen samples (Axelrod et al., 2021). Fig. 3 shows the relative contribution of different organic compounds for each pollen type grouped by chemical families: saccharides (α-glucose, β-glucose and sucrose), fatty acids (alpha-linoleic acid, linoleic acid, oleic acid, palmitic acid and stearic acid), amino acids (aspargine, glutamine, histidine and proline), diacids (azealic, glutaric, malic, succinic and tere-phthalic), ciclitols (pinitol, shikimic), anhydro-sugars (levoglucosan), plants compounds (oleanolic acid and sitosterol) and sugar-alcohols (mannitol and sorbitol).

The results show that the contribution of organic compounds among pollen types is highly variable (Fig. 3), which is consistent with recent studies (Axelrod et al., 2021; Mampage et al., 2022). Saccharides (α-glucose, β-glucose and sucrose) are the most prominent organic component in most of the pollen types, contributing over 80% in *Dactylis* (84.50%), *Fraxinus* (86.32%), and *Quercus* (87.57%). Among saccharides, *Fraxinus* and *Quercus* mainly contain α-glucose and β-glucose and their chemical compositions are quite similar, while sucrose dominates in *Dactylis*.

Amino acids are quite abundant organic components of *Populus nigra* (69.84%) and *Olea* 2021 (79.03%). *Populus deltoides* and *Acer* also show percentages of amino acids higher than 25%, but the contribution of amino acids to the rest of pollen types is lower than 10%. One of the most abundant amino acids in pollen grains is proline. We observe that its concentration is quite different between fresh *Olea* 2021 (55.33% of total measured organic compounds) and *Olea* 2019 (less than 7%). Proline is thought to have a protective role against environmental stress in addition to preserving pollen fertility (Trovato et al., 2019), however, it is a component that degrades as pollen ages (Mattioli et al., 2020) which might explain the degradation of *Olea* over time.

The results also show that fatty acids and diacids are also present in all pollen types but with varying contributions across types. Palmitic acid is the most abundant fatty acid in all pollen types, except for *Dactylis* where stearic acid is dominant. The overall low concentration of fatty acids in most pollen types could be attributed to absence of pollenkitt. Pollenkitt is the outermost layer of pollen (also called pollen coat) (Gong et al., 2015) and is composed mainly of lipids (as well as proteins and saccharides) (Ischebeck, 2016). It also has a sticky character which makes it more common in entomophilous plants (pollinated by insects) (Gong et al., 2015; Pacini and Hesse, 2005). However, it is not very common to find pollenkitt in anemophilous species (wind pollinated) which are the pollen types studied in this work. *Acer*, *Populus deltoides* and *Olea* 2019 show higher contribution of fatty acids compared with the rest of pollen types investigated. In contrast, *Quercus* has the lowest concentration. Previous studies concluded that fatty acids are generally hydrophobic (Broekhuizen et al., 2004; Pradeep Kumar et al., 2003) and they are characterised by low water activity (Haynes et al., 2016) therefore, they do not contribute significantly to water uptake (Nguyen et al., 2017), and are not likely to lead to CCN activity (Petters and Petters, 2016; Pradeep Kumar et al., 2003). Although we were not able to find any connection with the retrieved κ values, fatty acids have the ability to reduce surface tension at lower concentrations than other compounds (Petters and Petters, 2016), therefore, they could have a role in surface activity as discussed in Sect. 3.3.

Dactylis, *Fraxinus* and *Quercus*, have a similar amount of saccharides, but *Dactylis* shows a slightly higher κ value. This could be due to the presence of levoglucosan, which is not present in *Fraxinus* or *Quercus*. Rosenørn et al. (2006) found that the potential of disaccharides (such as sucrose) to nucleate cloud droplets is lower than the potential of monosaccharides (such as glucose) and levoglucosan (anhydro-sugar). Dawson et al. (2020) also obtained κ values of sucrose (0.10–0.15) lower than levoglucosan (0.20–0.30). However, *Dactilys* exhibits a higher contribution of sucrose, making it difficult to draw absolute conclusions on hygroscopicity based on the amount of these saccharides in the pollen samples.

Mikaihlov et al. (2021) suggested that the difficulty in finding a relationship between κ and organic concentration is related to the different solubility values of the organic compounds. SPPs are composed of both water-soluble components (such as sugars, proteins and inorganic ions) responsible for water uptake, and water-insoluble compounds (such as hydrosols or colloids), able to suppress hygroscopic growth and CCN activity. Our results have shown that SPPs consist of multiple organic compounds and their solubility values might be very different. The water solubility of each of these compounds (at 20 ℃ - 25 ℃) is shown in Table S1 and they have been classified as: (A) highly soluble (>700 mg/mL), (B) slightly soluble (0.5 mg/mL < solubility <700 mg/mL) and (C) non-soluble compounds (<0.5 mg/mL) according to Han et al. (2022). Following this criteria, we obtained the percentage of these categories with respect to the considered organic compounds as Petters and Kreidenweis (2008) suggested. The relation between the mean values of SPP hygroscopicity and the relative contribution of the organic compounds in terms of water-solubility is shown in Fig. 4.

Fig. 4 shows all κ values are in the same range (except *Quercus*) and there is not a clear relationship between hygroscopicity and chemical composition in terms of its solubility. Despite variations in the contribution of highly- and non-soluble constituents among species, the hygroscopicity parameter is similar. The slightly and highly soluble compounds exhibit a wide range for all pollen types, between 30% and 90% and from 8% to 66%, respectively. Therefore, non-soluble compounds make up less than 40%. Fig. 4 shows that SPPs composed of highly soluble constituents, such as *Dactylis*, exhibit similar hygroscopicity values as those found for SPPs with higher contribution of non-soluble compounds such as *Populus deltoides* or *Olea* 2019.Establishing a general relationship with the amount or contribution of soluble and non-soluble organic constituents in the pollen types analysed here requires further investigation. In contrast, studies based on single compounds (e.g., Pradeep Kumar et al., 2003) found clear relationships between solubility and κ, consistent with highly soluble organic particles being CCN active while the same size particle composed of an insoluble species would have low CCN activity. Riipinen et al. (2015) studied activation properties of multicomponent organic particles, and they concluded that hygroscopicity is related to water solubility in the range of slightly soluble species. However, Kuwata et al. (2013) showed molecular weight is the property that controls activation properties instead of solubility for highly soluble compounds. Wang et al. (2019) also concluded that the activation of most secondary organic aerosol (SOA) particles is related to molecular weight. SOA particles are formed from smaller VOCs molecules that tend to undergo oxidation and fragmentation leading to decreasing molecular weight and thus, increasing κ. We also explored the relationship between κ and molecular weight (not shown here), but the results were not conclusive since most pollen types exhibit similar hygroscopicity while estimated molecular weights had higher variability. Nevertheless, it should be mentioned that the results on the relationship between aerosol hygroscopicity, solubility and molecular weight are based on a selection of organic compounds and the bulk chemical composition is not fully recovered, which hampers the comparison. Further studies providing a more detail chemical speciation of SPPs could shed light on the relationship between solubility, molecular weight and hygroscopicity of primary organic aerosols.

3.3. Surface activity

Previous studies have evaluated the effect that surface tension (σ) might have on the CCN activation of organic aerosols (Prisle et al., 2019; Ruehl et al., 2010). To investigate the role of surface activity in cloud

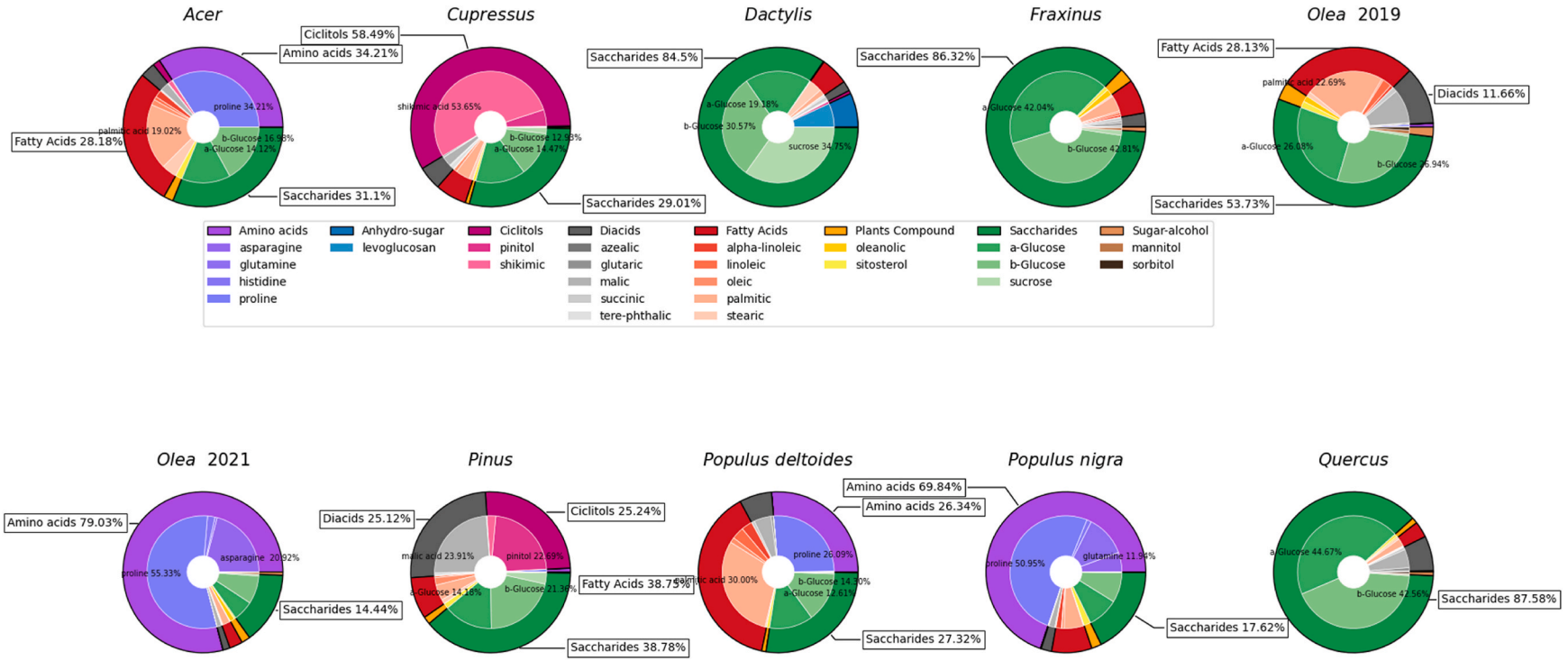

Fig. 3. Relative composition of individual molecular organic compounds and their groups for each pollen type (external ring). Only compounds representing percentages above 10% have been highlighted to appear in the pie charts.

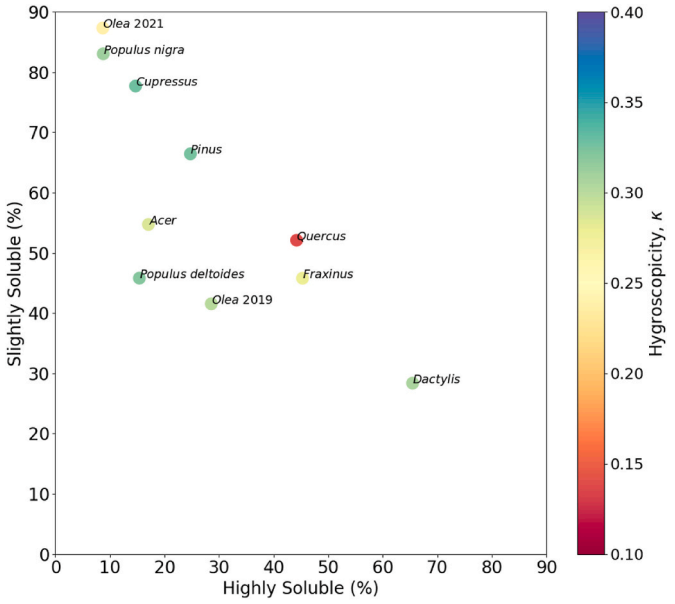

Fig. 4. Relative contribution of highly soluble and slightly soluble compounds in SPPs coloured by the hygroscopicity parameter κ for each pollen type.

droplet activation we measured the surface tension of different SPPs solutions (at different concentrations) for 6 pollen types (*Dactylis*, *Fraxinus*, *Pinus*, *Populus deltoides*, *Populus nigra* and *Quercus*) using Pendant Drop Tensiometry. The rest of the pollen types analysed in previous sections have not been considered in this analysis due to limited sample availability. As explained in Sect. 2.3, the filtration efficiency for each pollen type is different, thus, the initial concentrations calculated after filtration process were: 1.87 g/L, 1.43 g/L, 2.23 g/L, 1.83 g/L, 5.23 g/L and 1.05 g/L for *Populus deltoides, Populus nigra, Dactylis, Quercus, Pinus* and *Fraxinus*, respectively.

Fig. 5 shows the time evolution of surface tension at the initial concentration and at 1/10, 1/100 and 1/1000 of the initial concentration. The plots for *Dactylis, Fraxinus* and *Pinus* do not show the most diluted solutions because the other pollen types analysed demonstrate that if the measured surface tension remains close to surface tension of water (σ_W ~72.5 mN/m) over time, the more diluted solutions also exhibit σ_W values and do not change with time. All pollen types are surface active because the surface tension decreases in time for at least some solution concentrations. A lack of surface activity is indicated by surface tension values that are constant and similar to σ_w. However, the decreasing trend varies among species depending on pollen type and initial concentration. In general, the surface activity decreases as the initial solutions are diluted, consistent with recent results by Prisle et al. (2019).

At the initial concentrations, all pollen types analysed significantly reduce the surface tension over the course of the surface tension measurement. Interestingly, *Populus deltoides* is the only pollen type that reduces the surface tension at concentrations diluted 10 times. Finally, none of the pollen types are surface active at concentrations diluted 100 or 1000 times regardless of the initial concentration (Fig. 5). The reduction of surface tension is due to the adsorption of surface active compounds present in different pollen types and proceeds in two steps. A first period (<300 s) characterised by a rapid reduction of the surface tension and second phase in which the surface tension reaches a pseudo plateau (Nozière et al., 2014). For diluted solutions, the first period of the adsorption process is diffusion controlled and the rate of the surface tension reduction provides information on the diffusion of surface active compounds to the air-water surface. Conversely, highly concentrated solutions and/or highly surface active compounds begin with initial values of surface tension already low, indicating that the surface is already occupied by surface active compounds and the adsorption of new molecules encounters an energy barrier (Eastoe and Dalton, 2000). This is the case for the initial solution of *Populus deltoides* which shows surface tension values of 63.5 ± 1.5 mN/m, which is significantly lower than σ_w.

The decreasing rate of surface tension varies among species. Some pollen types, such as *Quercus* shows a decay curve of surface tension which is more linear with time than *Populus deltoides* or *Populus nigra* with similar initial concentrations. Table 3 shows the percentage of surface tension reduction during the first 300 s (time at which fast phase of decay is measurable and comparable between pollen species with fast

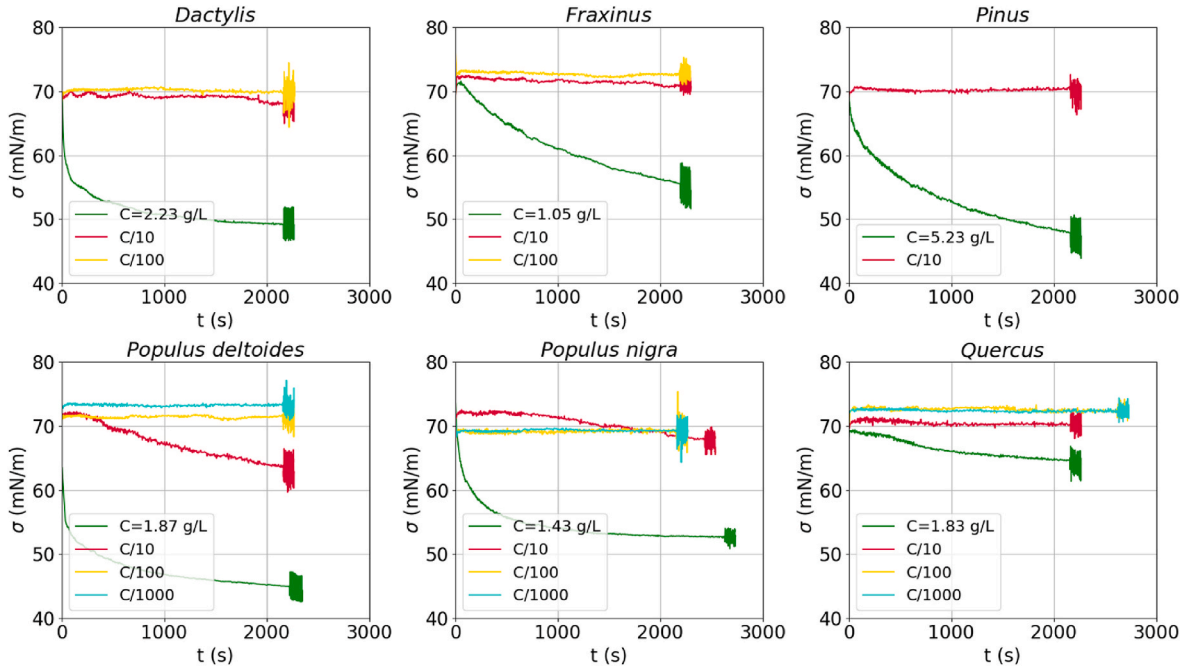

Fig. 5. *Surface tension versus time at different concentrations for Dactylis, Fraxinus, Pinus, Populus deltoides, Populus nigra* and *Quercus. Dilutions were made in ultrapure water, and measurements were made at room temperature (23 °C).*

Table 3
Percentage surface tension decrease at 300 s.

Pollen Type	Concentration (g/L)	% decrease in surface tension
Dactylis	C = 2.2 ± 0.4	22.0%
Fraxinus	C = 1.05 ± 0.08	6.6%
Pinus	C = 5.23 ± 0.06	14.9%
Populus deltoides	C = 1.9 ± 0.8	20.6%
	C/10	1.9%
Populus nigra	C = 1.4 ± 0.4	17.4%
	C/10	0%
Quercus	C = 1.8 ± 0.7	3.8%

and slow dynamical phases) for each SPP species for the concentrations at which they have been shown to be surface active. Comparison of the rate of surface tension reduction recorded for similar concentrations of approximately 1 g/L (Table 3) follows the order: *Populus deltoides* > *Populus nigra* > *Fraxinus* > *Quercus*, with *Populus deltoides* having the highest fatty acids concentration and *Quercus,* the lowest (Fig. 3). This could suggest that the surface active compounds may come principally from the free fatty acids.

After the initial rapid decay, the rate of surface tension reduction decreases until reaching a pseudo plateau indicative of saturation of the surface layer. However, not all pollen types reach a clear plateau during the experiment time (Fig. 5). At initial concentrations, *Dactylis, Quercus*, *Populus deltoides* and *Populus nigra* seem to be able to achieve this state, forming a surface layer characterised by surface tension values of 49.2 ± 1.5, 64.4 ± 1.5, 45.0 ± 1.5 and 52.7 ± 1.5 mN/m, respectively. However, *Fraxinus* (initial concentration), *Pinus* (initial concentration) and *Populus deltoides* (diluted 10 times) need more than ~2500 s to achieve it.

The last 200 s of the processes shown in Fig. 5 corresponds to dilatational rheology of adsorbed layers. It consists of inducing sinusoidal perturbations by injecting and extracting liquid into the droplet (Maldonado-Valderrama et al., 2005). This analysis provides information about the interfacial elasticity or viscosity, related to the response of the surface tension to area deformation (Decesari et al., 2003; Seidl, 2000) and is related to particle growth, kinetics and relaxation processes (not addressed in this study).

As it has been mentioned before, at the end of the adsorption kinetics curves, the surface tension reaches pseudo stable values indicative of the saturation of the surface layer (Fig. 5). The final values of surface tension are plotted in Fig. 6 versus SPP concentration in the solution. Error bars correspond to standard deviations of σ_W values obtained between each experiment. It should be mentioned that Fig. 6 only shows initial concentrations and concentrations diluted 10 and 100 times because Fig. 5 demonstrated that more diluted concentrations correspond to σ_w values. In the case of *Pinus,* the point representing the concentration diluted 100 times (open pink circle) is not an experimental value. It has been assumed to have the same surface tension value as the C/10 sample and has only been plotted to guide the eye and visualize the pattern easier.

The experimental results (Fig. 6) show again that the surface tension decreases for more concentrated solutions, while the surface tension approaches the value of water for more diluted solutions. However, as noted above, not all pollen types exhibit the same behaviour. Fig. 6 shows that the surface activity of all types of pollen analysed lie between the most surface active *Populus deltoides* and the least surface active *Quercus*. This is consistent with the amount of fatty acids found in these types (Fig. 3). Also, the shape of the surface tension curves plotted in Fig. 6 can provide additional information on the development of the surface layer by looking at both, the bulk concentration needed to reduce significantly the surface tension and, the lowest surface tension achieved by each of the pollen species. For concentrations between 1 g/L – 10 g/L, *Dactylis, Pinus* and *Populus deltoides* show surface tension values from 45 mN/m to 50 mN/m. *Populus nigra, Fraxinus* and *Quercus* reached 52.68 mN/m, 55.96 mN/m and 64.64 mN/m, respectively. For the range of concentrations between 0.1 g/L – 1 g/L, SPPs show surface tension

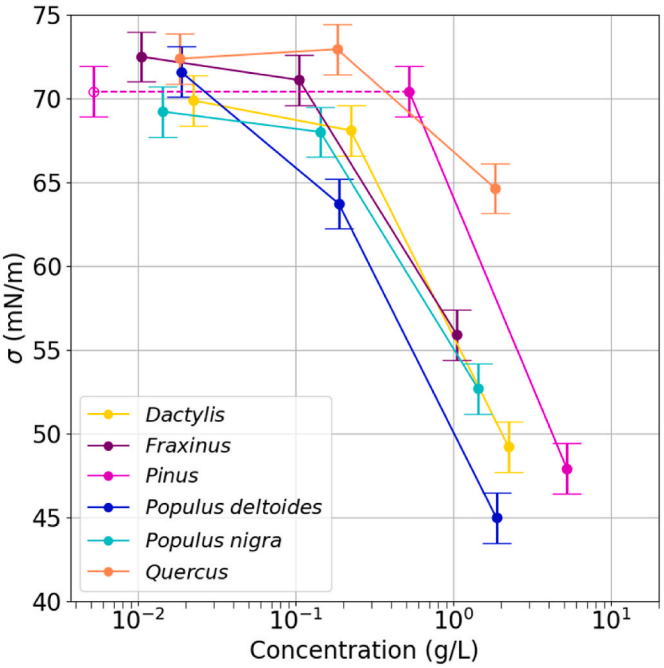

Fig. 6. Final values of surface tension after adsorption at constant surface area plotted in Fig. 5, as function of concentration for Dactylis, Fraxinus, Pinus, Populus deltoides, Populus nigra and Quercus. Error bars represent the standard deviation of the surface tension measured for pure water during the experiments.

values ranging from 60 mN/m to 72 mN/m. Finally, for concentrations lower than 0.1 g/L, surface tension values are found between 69 mN/m-72 mN/m, which are similar to σ_w. It should be highlighted that *Populus deltoides* requires the lowest bulk concentration needed to significantly reduce the surface tension and reaches the lowest value, hence it is the most surface active SPP type. In contrast, *Quercus* requires high bulk concentration to decrease σ, and still the final σ value reached remains high, indicative of a very diluted surface layer, and hence arises as the less surface active SPP type.

Petters and Petters (2016) showed that different surfactants groups do not have the same ability to reduce surface tension. Saccharides are not good surface tension reducers; they may even increase surface tension. This may be the reason for the low surface activity observed for *Quercus* (which has a chemical composition dominated by glucose). The surface activity of amino acids depends on their hydrophobicity/hydrophilicity (Kristensson et al., 2010; Raza et al., 2019); and the amino acids present in pollen are mostly hydrophilic. While *Fraxinus*, *Populus nigra*, *Pinus* and *Dactylis* contain similar amounts of fatty acids, the rest of their components are mostly non surface active, hence we cannot fully account for the surface activity shown in Fig. 6. Due to the limited number of pollen types investigated (6 in this case) and the similar behaviour and predominant organic composition of most of them, it is not possible to establish a clear relationship between composition and surface activity, although our findings suggest the presence of fatty acids could be related to the observed surface activity.

Our results have shown all SPP types act as surfactants, able to reduce surface tension. Nevertheless, this behaviour is strongly dependent on concentration, that is, pollen types tend to decrease surface tension when solutions are sufficiently concentrated but their impact on activation properties needs to be evaluated.

3.4. Impact of surface tension on hygroscopicity

To determine the impact of lowering the surface tension of SPP solutions on their hygroscopic properties, in the following we study how

the hygroscopic parameter κ varies with decreasing surface tension. SPPs clearly contain surface active compounds (likely related to fatty acids) because there is a reduction of surface tension, which might affect the derived hygroscopicity using Köhler theory. The experimental SS_{Crit} derived in Sect. 3.1 and the lowest surface tension values obtained above (instead of the water surface tension) have been used in Eq. (1) to recalculate the hygroscopicity parameter and to determine whether surface activity involves a significant impact on the ability of particles to activate as CCN, as previous studies suggest (Ovadnevaite et al., 2017; Ruehl et al., 2016).

According to Prisle et al. (2019) the concentration of SPP in cloud droplets is in the range of $10^{-5} - 2 \cdot 10^{-1}$ g/L and concentrations diluted C/100 fall within this range. The final surface tension values of these solutions are quite similar to σ_w (within the measurement uncertainties). However, in this study we can determine if slight variations in σ could be relevant for κ values. Results are shown in Fig. 7 and Table S2, indicating that κ values for the most concentrated solutions ($\kappa_{\sigma c}$) and at concentrations diluted 100 times ($\kappa_{\sigma c/100}$) are lower than the κ value obtained using water surface tension ($\kappa_{\sigma w}$) for all pollen types. Table S2 also shows the reduction percentage in the κ mean value (κ_{mean}).

All $\kappa_{\sigma C}$ are in the range 0.10–0.17 (for all particle dry diameters investigated 80, 100 and 200 nm) and the reduction in κ, relative to assuming the surface tension of water, is around 50–68%, except for *Quercus* (17.2%) and *Fraxinus* (39.3%). *Quercus* is the least surface active pollen type, with an equilibrium surface tension of 64.6 ± 1.5 mN/m (similar to σ_w). In contrast, *Populus deltoides* reached the lowest equilibrium surface tension (45.0 mN/m), and exhibited a strong reduction in κ.

Surfactant substances lead to reduced surface tension, decreasing the energetic barrier to equilibrium droplet growth, thus decreasing critical supersaturation (Davies et al., 2019) and leading to an overestimation of activation potential (Sorjamaa et al., 2004; Prisle et al., 2008). However, because the surfactant partitioning effect occurs, surfactants can migrate from the bulk to the surface, limiting the amount of dissolved solute in the droplet and thereby reducing water uptake capacity and κ (Fuentes et al., 2011; Sorjamaa et al., 2004).

For the κ values obtained using the modified surface tension values, in all cases there is a pronounced decrease in aerosol hygroscopicity for the most concentrated solutions (C). For solutions diluted 100 times from the initial concentration (C/100) the final σ values are similar to σ_w, resulting in a lesser impact on the κ values ($\kappa_{\sigma c/100}$ in Fig. 7). The percentage of reduction of mean $\kappa_{\sigma c/100}$ values is in the range 11.7–13.9% for all pollen types except for *Quercus* (1.5%) and all $\kappa_{\sigma c/100}$ values are within the error range of $\kappa_{\sigma w}$ values obtained.

In this study we focused on macroscopic droplets and concentrations that could be observed in atmospheric cloud droplets. Diluted concentrations reached surface tension values similar to σ_w. However, in microscopic droplets with high surface area to volume ratios, the partitioning of surface active compounds will deplete the bulk concentration as well as depress the surface tension of the droplet (Prisle et al., 2010). For a model system of Nordic Aquatic Fulvic Acid (NAFA) and NaCl, Lin et al. (2020) found that the surface tension depression and bulk depletion effects on cloud activation largely cancelled each other out. However, the extent to which that conclusion can be applied to other mixtures of atmospheric interest is unknown. Specifically, our results suggest that the minimal reduction in surface tension observed at low solute concentrations will not have a significant impact on whether SPPs activate as cloud condensation nuclei. However, more studies considering additional multicomponent organic aerosol particles (such as these different pollen types) where surface tension behaviour can be quite relevant, would be essential for further progress. Recent studies (Davies et al., 2019; Lin et al., 2020) point to the relevance of considering surface tension time-evolution in CCN activation suggesting further evaluation is necessary to draw more accurate conclusions.

4. Conclusions

We have studied different activation properties (critical supersaturation and hygroscopicity parameters), surface tension effects and organic composition of SPPs from 10 different Mediterranean pollen types. Our results demonstrated that subpollen particles (SPPs) of the most important Mediterranean species are able to activate at atmospherically-relevant supersaturations (0.07%–0.37%, depending on size). Hygroscopicity parameters, κ, obtained for each pollen type show that SPPs are classified as a moderately hygroscopic organic aerosol varying in the range between 0.23 and 0.33, except *Quercus* that

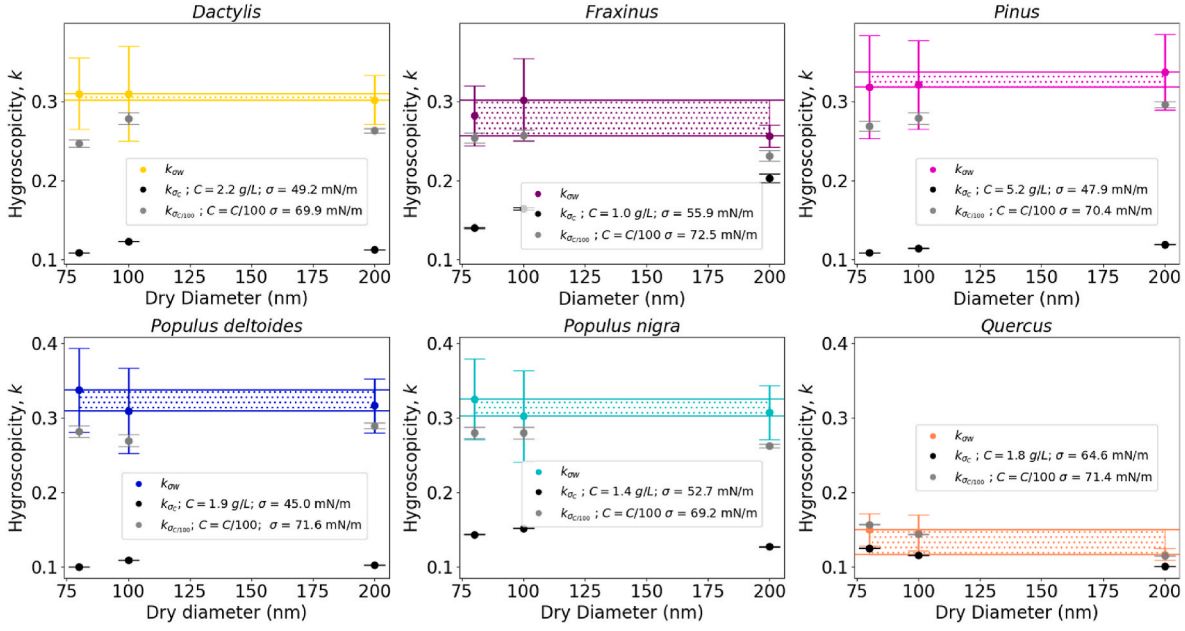

Fig. 7. κ values obtained using σ_w (noted as $\kappa_{\sigma w}$) and obtained with equilibrium surface tension values at highest concentrations ($\kappa_{\sigma C}$) and concentrations diluted 100 times ($\kappa_{\sigma C/100}$) for Dactylis, Fraxinus, Pinus, Populus deltoides, Populus nigra and Quercus. Horizontal lines represent maxima and minima values obtained for $\kappa_{\sigma w}$ and shaded area the interval between both values.

showed very low hygroscopicity (0.14). This suggests that SPPs might be an important natural contribution to the CCN budget. However, further studies are needed to determine more accurately how kinetic limitation in the CCN counter could affect the obtained activation properties of SPPs, although our results suggest they are within the range of *SS* measurements uncertainties.

Regarding chemical composition, our analysis show that total organic concentration and especially protein content is quite different among species. Saccharides are present in all analysed pollen types (α-glucose and β-glucose are the most abundant) although they show different relative contributions. The results also show a large variation of the composition of fatty acids among species, comprising nearly 40% of *Populus deltoides* and less than 5% in *Quercus*. Other chemicals such as amino acids and individual organic components also exhibit a great variability among species. The relative concentration of highly, slightly and non-soluble organic compounds varies among different types studied here (with very similar κ values), which could be the reason why the hygroscopic behaviour is not clearly related to water solubility.

Surface tension experiments reveal surface activity of all pollen types at high concentrations. *Populus deltoides* is the most surface active and *Quercus* is the least surface active. However, all SPPs from different pollen types are surface active at concentrations higher than 1 g/L. The surface activity reduces κ values by around 50%–60%, except for *Quercus* which only reduces κ values by 17.7%. The capacity to reduce surface tension decreases as SPP solution concentration decreases. If the SPP concentrations are lower than 0.03 g/L, surface tension values are similar to the surface tension of water (σ_w) and κ values are barely modified. Therefore, we can assume for low solution concentration, corresponding to those occurring during SPP activation, σ_w is a good approximation in the Köhler equation.

In summary, it is difficult to identify any relationships among κ, chemical composition and the surface activity of SPPs, at least for the pollen types investigated in this study. Our results suggest an increase in fatty acids contribution leads to higher surface activity when concentrations exceed 1 g/L. However, at low concentrations (suitable for cloud droplets) all SPPs are practically non-surface active, independently of chemical composition.

Previous research with single organic components provides insightful results on the CCN activation properties of different organic compounds such as fatty acids, amino acids or saccharides, however our study is focused on atmospheric pollen samples, composed of multiple different chemical compounds, which makes it very difficult to draw conclusive results. We have seen that all these pollen types, except *Quercus,* exhibit similar activation properties, suggesting that their behaviour is quite similar in terms of activation and cloud droplet formation. Comprehensive studies including new SPPs types, typical in different regions and chemical analysis should be performed in order to improve the understanding of activation and hygroscopic properties of SPPs.

Due to the forecasted increase in pollen release with climate change, and the large SPP generation potential of each pollen grain, further research and additional physical and chemical properties should be studied to better understand the factors controlling SPPs activation properties.

CRediT authorship contribution statement

A. Casans: Conceptualization, Investigation, Methodology, Data curation, Writing – original draft, Visualization. **F. Rejano:** Conceptualization, Investigation, Methodology, Writing – review & editing. **J. Maldonado-Valderrama:** Methodology, Investigation, Writing – review & editing. **J.A. Casquero-Vera:** Conceptualization, Data curation, Formal analysis, Writing – review & editing. **S. Ruiz-Peñuela:** Methodology, Writing – review & editing. **B.L. van Drooge:** Methodology, Writing – review & editing. **H. Lyamani:** Conceptualization, Resources. **A. Cazorla:** Writing – review & editing. **E. Andrews:** Writing – review & editing. **Jack J. Lin:** Conceptualization, Writing – review & editing. **F. Mirza-Montoro:** Conceptualization, Resources. **D. Pérez-Ramírez:** Writing – review & editing. **F.J. Olmo:** Writing – review & editing, Funding acquisition. **L. Alados-Arboledas:** Writing – review & editing, Funding acquisition. **P. Cariñanos:** Resources, Writing – review & editing. **G. Titos:** Supervision, Conceptualization, Investigation, Methodology, Project administration, Writing – review & editing, Funding acquisition.

Declaration of competing interest

The authors declare that they have no known competing financial interests or personal relationships that could have appeared to influence the work reported in this paper.

Data availability

Data will be made available on request.

Acknowledgements

This work was supported by BioCloud project (RTI2018.101154.A.I00) funded by MCIN/AEI/10.13039/501100011033, FEDER "Una manera de hacer Europa" and NUCLEUS project (PID2021-128757OB-I00) funded by MCIN/AEI/10.13039/501100011033 and NextGenerationEU/PRTR. This work received support from the European Union's Horizon 2020 research and innovation program through projects ACTRIS.IMP (grant agreement No 871115) and ATMO_ACCESS (grant agreement No 101008004), by the Spanish Ministry of Science and Innovation through projects ELPIS (PID2020-120015RB-I00) and ACTRIS-España (CGL2017-90884REDT)). By the Junta de Andalucía Excellence, project ADPANE (P20-00136), AEROPRE (P-18-RT-3820) and by University of Granada Plan Propio through Visiting Scholars (PPVS2018-04), Singular Laboratory (LS2022-1) programs and Pre-Competitive Research Projects Pre-Greenmitigation3 (PP2022.PP34). Funding for open access charge, University of Granada/CBUA. Andrea Casans is funded by Spanish ministry of research and innovation under the predoctoral program FPI (PRE2019-090827) funded by MCIN/AEI/10.13039/501100011033, FSE "El FSE invierte en tu futuro". Fernando Rejano is funded by Spanish ministry of universities through predoctoral grant FPU19/05340. Juan Andrés Casquero-Vera is funded by FJC2021-047873-I, MCIN/AEI/10.13039/501100011033 and NextGenerationEU/PRTR. Elisabeth Andrews is funded in part by NOAA cooperative agreements NA17OAR4320101. Thanks to the NOAA Global Monitoring Laboratory for the use of the CCN counter.

Appendix A. Supplementary data

Supplementary data to this article can be found online at https://doi.org/10.1016/j.atmosenv.2023.119961.

References

Abbatt, J.P.D., Broekhuizen, K., Pradeep Kumar, P., 2005. Cloud condensation nucleus activity of internally mixed ammonium sulfate/organic acid aerosol particles. Atmos. Environ. 39, 4767–4778. https://doi.org/10.1016/j.atmosenv.2005.04.029.

Andreae, M.O., Rosenfeld, D., 2008. Aerosol cloud precipitation interactions. Part 1. The nature and sources of cloud-active aerosols. Earth Sci. Rev. 89, 13–41.

Axelrod, K., Samburova, V., Khlystov, A.Y., 2021. Relative abundance of saccharides, free amino acids, and other compounds in specific pollen species for source profiling of atmospheric aerosol. Sci. Total Environ. 799, 149254 https://doi.org/10.1016/j.scitotenv.2021.149254.

Berry, J.D., Neeson, M.J., Dagastine, R.R., Chan, D.Y.C., Tabor, R.F., 2015. Measurement of surface and interfacial tension using pendant drop tensiometry. J. Colloid Interface Sci. 454, 226–237. https://doi.org/10.1016/j.jcis.2015.05.012.

Bougiatioti, A., Argyrouli, A., Solomos, S., Vratolis, S., Eleftheriadis, K., Papayannis, A., Nenes, A., 2017. CCN activity, variability and influence on droplet formation during the HygrA-Cd campaign in athens. Atmosphere 8, 108. https://doi.org/10.3390/atmos8060108.

Bradford, M.M., 1976. A rapid and sensitive method for the quantitation of microgram quantities of protein utilizing the principle of protein-dye binding. Anal. Biochem. 72, 248–254. https://doi.org/10.1016/0003-2697(76)90527-3.

Broekhuizen, K.E., Thornberry, T., Kumar, P.P., Abbatt, J.P.D., 2004. Formation of cloud condensation nuclei by oxidative processing: unsaturated fatty acids. J. Geophys. Res. Atmos. 109 https://doi.org/10.1029/2004JD005298.

Burgos, M.A., Andrews, E., Titos, G., Benedetti, A., Bian, H., Buchard, V., Curci, G., Kipling, Z., Kirkevåg, A., Kokkola, H., Laakso, A., Letertre-Danczak, J., Lund, M.T., Matsui, H., Myhre, G., Randles, C., Schulz, M., van Noije, T., Zhang, K., Alados-Arboledas, L., Baltensperger, U., Jefferson, A., Sherman, J., Sun, J., Weingartner, E., Zieger, P., 2020. A global model–measurement evaluation of particle light scattering coefficients at elevated relative humidity. Atmos. Chem. Phys. 20, 10231–10258. https://doi.org/10.5194/acp-20-10231-2020.

Burkart, J., Gratzl, J., Seifried, T.M., Bieber, P., Grothe, H., 2021. Isolation of subpollen particles (SPPs) of birch: SPPs are potential carriers of ice nucleating macromolecules. Biogeosciences 18, 5751–5765. https://doi.org/10.5194/bg-18-5751-2021.

Cabrerizo-Vílchez, M.A., Wege, H.A., Holgado-Terriza, J.A., Neumann, A.W., 1999. Axisymmetric drop shape analysis as penetration Langmuir balance. Rev. Sci. Instrum. 70, 2438–2444. https://doi.org/10.1063/1.1149773.

Cariñanos, P., Guerrero-Rascado, J.L., Valle, A.M., Cazorla, A., Titos, G., Foyo-Moreno, I., Alados-Arboledas, L., Díaz de la Guardia, C., 2022. Assessing pollen extreme events over a Mediterranean site: role of local surface meteorology. Atmos. Environ. 272, 118928 https://doi.org/10.1016/j.atmosenv.2021.118928.

Cariñanos, P., Ruiz-Peñuela, S., Valle, A.M., de la Guardia, C.D., 2020. Assessing pollination disservices of urban street-trees: the case of London-plane tree (Platanus x hispanica Mill. ex Münchh). Sci. Total Environ. 737, 139722 https://doi.org/10.1016/j.scitotenv.2020.139722.

Chen, J., Budisulistiorini, S.H., Miyakawa, T., Komazaki, Y., Kuwata, M., 2018. Secondary aerosol formation promotes water uptake by organic-rich wildfire haze particles in equatorial Asia. Atmos. Chem. Phys. 18, 7781–7798. https://doi.org/10.5194/acp-18-7781-2018.

Davies, J.F., Zuend, A., Wilson, K.R., 2019. Technical note: the role of evolving surface tension in the formation of cloud droplets. Atmos. Chem. Phys. 19, 2933–2946. https://doi.org/10.5194/acp-19-2933-2019.

Dawson, J.N., Malek, K.A., Razafindrambinina, P.N., Raymond, T.M., Dutcher, D.D., Asa-Awuku, A.A., Freedman, M.A., 2020. Direct comparison of the submicron aerosol hygroscopicity of water-soluble sugars. ACS Earth Sp. Chem. 4, 2215–2226. https://doi.org/10.1021/acsearthspacechem.0c00159.

Decesari, S., Facchini, M.C., Mircea, M., Cavalli, F., Fuzzi, S., 2003. Solubility properties of surfactants in atmospheric aerosol and cloud/fog water samples. J. Geophys. Res. Atmos. 108 https://doi.org/10.1029/2003JD003566.

Deguillaume, L., Leriche, M., Amato, P., Ariya, P.A., Delort, A.-M., Pöschl, U., Chaumerliac, N., Bauer, H., Flossmann, A.I., Morris, C.E., 2008. Microbiology and atmospheric processes: chemical interactions of primary biological aerosols. Biogeosciences 5, 1073–1084. https://doi.org/10.5194/bg-5-1073-2008.

Després, V., Huffman, J.A., Burrows, S.M., Hoose, C., Safatov, A., Buryak, G., Fröhlich-Nowoisky, J., Elbert, W., Andreae, M., Pöschl, U., Jaenicke, R., 2012. Primary biological aerosol particles in the atmosphere: a review. Tellus B 64, 15598. https://doi.org/10.3402/tellusb.v64i0.15598.

Dusek, U., Frank, G.P., Curtius, J., Drewnick, F., Schneider, J., Kürten, A., Rose, D., Andreae, M.O., Borrmann, S., Pöschl, U., 2010. Enhanced organic mass fraction and decreased hygroscopicity of cloud condensation nuclei (CCN) during new particle formation events. Geophys. Res. Lett. 37 https://doi.org/10.1029/2009GL040930.

Dusek, U., Frank, G.P., Hildebrandt, L., Curtius, J., Schneider, J., Walter, S., Chand, D., Drewnick, F., Hings, S., Jung, D., Borrmann, S., Andreae, M.O., 2006. Size matters more than chemistry for cloud-nucleating ability of aerosol particles. Science 312, 1375–1378. https://doi.org/10.1126/science.1125261.

Eastoe, J., Dalton, J.S., 2000. Dynamic surface tension and adsorption mechanisms of surfactants at the air–water interface. Adv. Colloid Interface Sci. 85, 103–144. https://doi.org/10.1016/S0001-8686(99)00017-2.

Ervens, B., Cubison, M.J., Andrews, E., Feingold, G., Ogren, J.A., Jimenez, J.L., Quinn, P. K., Bates, T.S., Wang, J., Zhang, Q., Coe, H., Flynn, M., Allan, J.D., 2010. CCN predictions using simplified assumptions of organic aerosol composition and mixing state: a synthesis from six different locations. Atmos. Chem. Phys. 10, 4795–4807. https://doi.org/10.5194/acp-10-4795-2010.

Fontal, M., van Drooge, B.L., López, J.F., Fernández, P., Grimalt, J.O., 2015. Broad spectrum analysis of polar and apolar organic compounds in submicron atmospheric particles. J. Chromatogr. A 1404, 28–38. https://doi.org/10.1016/j.chroma.2015.05.042.

Forestieri, S.D., Staudt, S.M., Kuborn, T.M., Faber, K., Ruehl, C.R., Bertram, T.H., Cappa, C.D., 2018. \hack{\vskip-4mm}Establishing the impact of model surfactants on cloud condensation nuclei activity of sea spray aerosol mimics. Atmos. Chem. Phys. 18, 10985–11005. https://doi.org/10.5194/acp-18-10985-2018.

Fraga, H., Moriondo, M., Leolini, L., Santos, J.A., 2021. Mediterranean olive orchards under climate change: a review of future impacts and adaptation strategies. Agronomy 11. https://doi.org/10.3390/agronomy11010056.

Fröhlich-Nowoisky, J., Kampf, C.J., Weber, B., Huffman, J.A., Pöhlker, C., Andreae, M. O., Lang-Yona, N., Burrows, S.M., Gunthe, S.S., Elbert, W., Su, H., Hoor, P., Thines, E., Hoffmann, T., Després, V.R., Pöschl, U., 2016. Bioaerosols in the Earth system: climate, health, and ecosystem interactions. Atmos. Res. 182, 346–376. https://doi.org/10.1016/j.atmosres.2016.07.018.

Fuentes, E., Coe, H., Green, D., McFiggans, G., 2011. On the impacts of phytoplankton-derived organic matter on the properties of the primary marine aerosol – Part 2: composition, hygroscopicity and cloud condensation activity. Atmos. Chem. Phys. 11, 2585–2602. https://doi.org/10.5194/acp-11-2585-2011.

Gong, F., Wu, X., Wang, W., 2015. Diversity and function of maize pollen coat proteins: from biochemistry to proteomics. Front. Plant Sci. 6 https://doi.org/10.3389/fpls.2015.00199.

Grote, M., Valenta, R., Reichelt, R., 2003. Abortive pollen germination: a mechanism of allergen release in birch, alder, and hazel revealed by immunogold electron microscopy. J. Allergy Clin. Immunol. 111, 1017–1023. https://doi.org/10.1067/mai.2003.1452.

Guerrero, N., López, M., Caudullo, G., de Rigo, D., 2016. Olea Europaea in Europe: Distribution, Habitat, Usage and Threats.

Gysel, M., Weingartner, E., Baltensperger, U., 2002. Hygroscopicity of aerosol particles at low temperatures. 2. Theoretical and experimental hygroscopic properties of laboratory generated aerosols. Environ. Sci. Technol. 36, 63–68. https://doi.org/10.1021/es010055g.

Han, S., Hong, J., Luo, Q., Xu, H., Tan, H., Wang, Q., Tao, J., Zhou, Y., Peng, L., He, Y., Shi, J., Ma, N., Cheng, Y., Su, H., 2022. Hygroscopicity of organic compounds as a function of organic functionality, water solubility, molecular weight, and oxidation level. Atmos. Chem. Phys. 22, 3985–4004. https://doi.org/10.5194/acp-22-3985-2022.

Haynes, W.M., Lide, D.R., Bruno, T.J., 2016. CRC Handbook of Chemistry and Physics, 97th ed. https://doi.org/10.1201/9781315380476.

Hoorfar, M., Neumann, A.W., 2006. Recent progress in axisymmetric drop shape analysis (ADSA). Adv. Colloid Interface Sci. 121, 25–49. https://doi.org/10.1016/j.cis.2006.06.001.

Hoose, C., Kristjánsson, J., Burrows, S., 2010. How important is biological ice nucleation in clouds on a global scale? Environ. Res. Lett. v. 5, 5. https://doi.org/10.1088/1748-9326/5/2/024009.

Hoose, C., Möhler, O., 2012. Heterogeneous ice nucleation on atmospheric aerosols: a review of results from laboratory experiments. Atmos. Chem. Phys. 12, 9817–9854. https://doi.org/10.5194/acp-12-9817-2012.

Hughes, D.D., Mampage, C.B.A., Jones, L.M., Liu, Z., Stone, E.A., 2020. Characterization of atmospheric pollen fragments during springtime thunderstorms. Environ. Sci. Technol. Lett. 7, 409–414. https://doi.org/10.1021/acs.estlett.0c00213.

Ischebeck, T., 2016. Lipids in pollen — they are different. Biochim. Biophys. Acta, Mol. Cell Biol. Lipids 1861, 1315–1328. https://doi.org/10.1016/j.bbalip.2016.03.023.

Kanakidou, M., Seinfeld, J.H., Pandis, S.N., Barnes, I., Dentener, F.J., Facchini, M.C., Van Dingenen, R., Ervens, B., Nenes, A., Nielsen, C.J., Swietlicki, E., Putaud, J.P., Balkanski, Y., Fuzzi, S., Horth, J., Moortgat, G.K., Winterhalter, R., Myhre, C.E.L., Tsigaridis, K., Vignati, E., Stephanou, E.G., Wilson, J., 2005. Organic aerosol and global climate modelling: a review. Atmos. Chem. Phys. 5, 1053–1123. https://doi.org/10.5194/acp-5-1053-2005.

Köhler, H., 1936. The nucleus in and the growth of hygroscopic droplets. Trans. Faraday Soc. 32, 1152–1161. https://doi.org/10.1039/TF9363201152.

Krajter Ostoić, S., Salbitano, F., Borelli, S., Verlič, A., 2018. Urban forest research in the Mediterranean: a systematic review. Urban For. Urban Green. 31, 185–196. https://doi.org/10.1016/j.ufug.2018.03.005.

Kristensson, A., Rosenørn, T., Bilde, M., 2010. Cloud droplet activation of amino acid aerosol particles. J. Phys. Chem. A 114, 379–386. https://doi.org/10.1021/jp9055329.

Kuwata, M., Shao, W., Lebouteiller, R., Martin, S.T., 2013. Classifying organic materials by oxygen-to-carbon elemental ratio to predict the activation regime of Cloud Condensation Nuclei (CCN). Atmos. Chem. Phys. 13, 5309–5324. https://doi.org/10.5194/acp-13-5309-2013.

Lance, S., Nenes, A., Medina, J., Smith, J.N., 2006. Mapping the operation of the DMT continuous flow CCN counter. Aerosol Sci. Technol. 40, 242–254. https://doi.org/10.1080/02786820500543290.

Lawson, S.P., Kennedy, K.B., Rehan, S.M., 2021. Pollen composition significantly impacts the development and survival of the native small carpenter bee, Ceratina calcarata. Ecol. Entomol. 46, 232–239. https://doi.org/10.1111/een.12955.

Lin, J.J., Kristensen, T.B., Calderón, S.M., Malila, J., Prisle, N.L., 2020. Effects of surface tension time-evolution for CCN activation of a complex organic surfactant. Environ. Sci. Process. Impacts 22, 271–284. https://doi.org/10.1039/C9EM00426B.

Maldonado-Valderrama, J., del Castillo-Santaella, T., Gálvez-Ruiz, M.J., Holgado-Terriza, J.A., Cabrerizo-Vílchez, M.Á., 2021. In: Chapter 1 - Structure and Functionality of Interfacial Layers in Food Emulsions. Academic Press, pp. 1–22. https://doi.org/10.1016/B978-0-12-821453-4.00010-7.

Maldonado-Valderrama, J., Fainerman, V.B., Gálvez-Ruiz, M.J., Martín-Rodriguez, A., Cabrerizo-Vílchez, M.A., Miller, R., 2005. Dilatational rheology of β-casein adsorbed layers at Liquid−Fluid interfaces. J. Phys. Chem. B 109, 17608–17616. https://doi.org/10.1021/jp050927r.

Maldonado-Valderrama, J., Martín-Molina, A., Gálvez-Ruiz, M.J., Martín-Rodríguez, A., Cabrerizo-Vílchez, M.Á., 2004. β-Casein adsorption at liquid interfaces: theory and experiment. J. Phys. Chem. B 108, 12940–12945. https://doi.org/10.1021/jp048388y.

Mampage, C.B.A., Hughes, D.D., Jones, L.M., Metwali, N., Thorne, P.S., Stone, E.A., 2022. Characterization of sub-pollen particles in size-resolved atmospheric aerosol using chemical tracers. Atmos. Environ. X 15, 100177. https://doi.org/10.1016/j.aeaoa.2022.100177.

Manninen, H., Bäck, J., Sihto-Nissilä, S.-L., Huffman, J., Pessi, A.-M., Hiltunen, V., Aalto, P., Hidalgo, P., Hari, P., Saarto, A., Kulmala, M., Petäjä, T., 2014. Patterns in airborne pollen and other primary biological aerosol particles (PBAP), and their contribution to aerosol mass and number in a boreal forest. Boreal Environ. Res. 19, 383–405.

Mattioli, R., Palombi, N., Funck, D., Trovato, M., 2020. Proline accumulation in pollen grains as potential target for improved yield stability under salt stress. Front. Plant Sci. 11 https://doi.org/10.3389/fpls.2020.582877.

Medeiros, P.M., Simoneit, B.R.T., 2007. Analysis of sugars in environmental samples by gas chromatography–mass spectrometry. J. Chromatogr. A 1141, 271–278. https://doi.org/10.1016/j.chroma.2006.12.017.

Mei, F., Hayes, P.L., Ortega, A., Taylor, J.W., Allan, J.D., Gilman, J., Kuster, W., de Gouw, J., Jimenez, J.L., Wang, J., 2013. Droplet activation properties of organic aerosols observed at an urban site during CalNex-LA. J. Geophys. Res. Atmos. 118, 2903–2917. https://doi.org/10.1002/jgrd.50285.

Mikhailov, E.F., Ivanova, O.A., Nebosko, E.Y., Vlasenko, S.S., Ryshkevich, T.I., 2019. Subpollen particles as atmospheric cloud condensation nuclei. Izvestiya Atmos. Ocean. Phys. 55, 357–364. https://doi.org/10.1134/S000143381904008X.

Mikhailov, E.F., Pöhlker, M.L., Reinmuth-Selzle, K., Vlasenko, S.S., Krüger, O.O., Fröhlich-Nowoisky, J., Pöhlker, C., Ivanova, O.A., Kiselev, A.A., Kremper, L.A., Pöschl, U., 2021. Water uptake of subpollen aerosol particles: hygroscopic growth, cloud condensation nuclei activation, and liquid–liquid phase separation. Atmos. Chem. Phys. 21, 6999–7022. https://doi.org/10.5194/acp-21-6999-2021.

Molina, J.A., Martín-Sanz, J.P., Valverde-Asenjo, I., Sánchez-Jiménez, A., Quintana, J.R., 2023. Mediterranean grassland succession as an indicator of changes in ecosystem biodiversity and functionality. Biodivers. Conserv. 32, 95–118. https://doi.org/10.1007/s10531-022-02481-y.

Nguyen, Q.T., Kjær, K.H., Kling, K.I., Boesen, T., Bilde, M., 2017. Impact of fatty acid coating on the CCN activity of sea salt particles. Tellus B 69, 1304064. https://doi.org/10.1080/16000889.2017.1304064.

Nozière, B., Baduel, C., Jaffrezo, J.-L., 2014. The dynamic surface tension of atmospheric aerosol surfactants reveals new aspects of cloud activation. Nat. Commun. 5, 3335. https://doi.org/10.1038/ncomms4335.

Oros, D.R., Simoneit, B.R.T., 2001. Identification and emission factors of molecular tracers in organic aerosols from biomass burning Part 1. Temperate climate conifers. Appl. Geochem. 16, 1513–1544. https://doi.org/10.1016/S0883-2927(01)00021-X.

Ovadnevaite, J., Zuend, A., Laaksonen, A., Sanchez, K.J., Roberts, G., Ceburnis, D., Decesari, S., Rinaldi, M., Hodas, N., Facchini, M.C., Seinfeld, J.H., O' Dowd, C., 2017. Surface tension prevails over solute effect in organic-influenced cloud droplet activation. Nature 546, 637–641. https://doi.org/10.1038/nature22806.

Pacini, E., Guarnieri, M., Nepi, M., 2006. Pollen carbohydrates and water content during development, presentation, and dispersal: a short review. Protoplasma 228, 73. https://doi.org/10.1007/s00709-006-0169-z.

Pacini, E., Hesse, M., 2005. Pollenkitt - its composition, forms and functions. Flora - Morphol. Distrib. Funct. Ecol. Plants 200, 399–415. https://doi.org/10.1016/j.flora.2005.02.006.

Petters, M.D., Kreidenweis, S.M., 2013. A single parameter representation of hygroscopic growth and cloud condensation nucleus activity – Part 3: including surfactant partitioning. Atmos. Chem. Phys. 13, 1081–1091. https://doi.org/10.5194/acp-13-1081-2013.

Petters, M.D., Kreidenweis, S.M., 2008. A single parameter representation of hygroscopic growth and cloud condensation nucleus activity – Part 2: including solubility. Atmos. Chem. Phys. 8, 6273–6279. https://doi.org/10.5194/acp-8-6273-2008.

Petters, M.D., Kreidenweis, S.M., 2007. A single parameter representation of hygroscopic growth and cloud condensation nucleus activity. Atmos. Chem. Phys. 7, 1961–1971. https://doi.org/10.5194/acp-7-1961-2007.

Petters, S.S., Petters, M.D., 2016. Surfactant effect on cloud condensation nuclei for two-component internally mixed aerosols. J. Geophys. Res. Atmos. 121, 1878–1895. https://doi.org/10.1002/2015JD024090.

Pöhlker, M.L., Pöhlker, C., Ditas, F., Klimach, T., de Angelis, I., Araújo, A., Brito, J., Carbone, S., Cheng, Y., Chi, X., Ditz, R., Gunthe, S.S., Kesselmeier, J., Könemann, T., Lavrič, J.V., Martin, S.T., Mikhailov, E., Moran-Zuloaga, D., Rose, D., Saturno, J., Su, H., Thalman, R., Walter, D., Wang, J., Wolff, S., Barbosa, H.M.J., Artaxo, P., Andreae, M.O., Pöschl, U., 2016. Long-term observations of cloud condensation nuclei in the Amazon rain forest – Part 1: aerosol size distribution, hygroscopicity, and new model parametrizations for CCN prediction. Atmos. Chem. Phys. 16, 15709–15740. https://doi.org/10.5194/acp-16-15709-2016.

Pope, F.D., 2010. Pollen grains are efficient cloud condensation nuclei. Environ. Res. Lett. 5, 44015 https://doi.org/10.1088/1748-9326/5/4/044015.

Pöschl, U., Martin, S.T., Sinha, B., Chen, Q., Gunthe, S.S., Huffman, J.A., Borrmann, S., Farmer, D.K., Garland, R.M., Helas, G., Jimenez, J.L., King, S.M., Manzi, A., Mikhailov, E., Pauliquevis, T., Petters, M.D., Prenni, A.J., Roldin, P., Rose, D., Schneider, J., Su, H., Zorn, S.R., Artaxo, P., Andreae, M.O., 2010. Rainforest aerosols as biogenic nuclei of clouds and precipitation in the Amazon. Science 329, 1513–1516. https://doi.org/10.1126/science.1191056.

Pradeep Kumar, P., Broekhuizen, K., Abbatt, J.P.D., 2003. Organic acids as cloud condensation nuclei: laboratory studies of highly soluble and insoluble species. Atmos. Chem. Phys. 3, 509–520. https://doi.org/10.5194/acp-3-509-2003.

Prisle, N.L., Lin, J.J., Purdue, S., Lin, H., Meredith, J.C., Nenes, A., 2019. Cloud condensation nuclei activity of six pollenkitts and the influence of their surface activity. Atmos. Chem. Phys. 19, 4741–4761. https://doi.org/10.5194/acp-19-4741-2019.

Prisle, N.L., Raatikainen, T., Laaksonen, A., Bilde, M., 2010. Surfactants in cloud droplet activation: mixed organic-inorganic particles. Atmos. Chem. Phys. 10, 5663–5683. https://doi.org/10.5194/acp-10-5663-2010.

Prisle, N.L., Raatikainen, T., Sorjamaa, R., Svenningsson, B., Laaksonen, A.R.I., Bilde, M., 2008. Surfactant partitioning in cloud droplet activation: a study of C8, C10, C12 and C14 normal fatty acid sodium salts. Tellus B 60, 416–431. https://doi.org/10.1111/j.1600-0889.2008.00352.x.

Pummer, B.G., Bauer, H., Bernardi, J., Bleicher, S., Grothe, H., 2012. Suspendable macromolecules are responsible for ice nucleation activity of birch and conifer pollen. Atmos. Chem. Phys. 12, 2541–2550. https://doi.org/10.5194/acp-12-2541-2012.

Quinn, P.K., Bates, T.S., Baynard, T., Clarke, A.D., Onasch, T.B., Wang, W., Rood, M.J., Andrews, E., Allan, J., Carrico, C.M., Coffman, D., Worsnop, D., 2005. Impact of particulate organic matter on the relative humidity dependence of light scattering: a simplified parameterization. Geophys. Res. Lett. 32 https://doi.org/10.1029/2005GL024322.

Rama, H.-O., Roberts, D., Tignor, M., Poloczanska, E.S., Mintenbeck, K., Alegría, A., Craig, M., Langsdorf, S., Löschke, S., Möller, V., Okem, A., Rama, B., Ayanlade, S., 2022. Climate change 2022: impacts, adaptation and vulnerability working group II contribution to the sixth assessment report of the intergovernmental panel on climate change. https://doi.org/10.1017/9781009325844.

Rathnayake, C.M., Metwali, N., Jayarathne, T., Kettler, J., Huang, Y., Thorne, P.S., O'Shaughnessy, P.T., Stone, E.A., 2017. Influence of rain on the abundance of bioaerosols in fine and coarse particles. Atmos. Chem. Phys. 17, 2459–2475. https://doi.org/10.5194/acp-17-2459-2017.

Raymond, T.M., Pandis, S.N., 2002. Cloud activation of single-component organic aerosol particles. J. Geophys. Res. Atmos. 107 https://doi.org/10.1029/2002JD002159. AAC 16-1-AAC 16-8.

Raza, M.A., Hallett, P.D., Liu, X., He, M., Afzal, W., 2019. Surface tension of aqueous solutions of small-chain amino and organic acids. J. Chem. Eng. Data 64, 5049–5056. https://doi.org/10.1021/acs.jced.9b00026.

Rejano, F., Titos, G., Casquero-Vera, J.A., Lyamani, H., Andrews, E., Sheridan, P., Cazorla, A., Castillo, S., Alados-Arboledas, L., Olmo, F.J., 2021. Activation properties of aerosol particles as cloud condensation nuclei at urban and high-altitude remote sites in southern Europe. Sci. Total Environ. 762, 143100 https://doi.org/10.1016/j.scitotenv.2020.143100.

Riipinen, I., Rastak, N., Pandis, S.N., 2015. Connecting the solubility and CCN activation of complex organic aerosols: a theoretical study using solubility distributions. Atmos. Chem. Phys. 15, 6305–6322. https://doi.org/10.5194/acp-15-6305-2015.

Rissanen, T., Hyötyläinen, T., Kallio, M., Kronholm, J., Kulmala, M., Riekkola, M.-L., 2006. Characterization of organic compounds in aerosol particles from a coniferous forest by GC–MS. Chemosphere 64, 1185–1195. https://doi.org/10.1016/j.chemosphere.2005.11.079.

Roberts, G.C., Nenes, A., 2005. A continuous-flow streamwise thermal-gradient CCN chamber for atmospheric measurements. Aerosol Sci. Technol. 39, 206–221. https://doi.org/10.1080/027868290913988.

Rose, D., Gunthe, S.S., Mikhailov, E., Frank, G.P., Dusek, U., Andreae, M.O., Pöschl, U., 2008. Calibration and measurement uncertainties of a continuous-flow cloud condensation nuclei counter (DMT-CCNC): CCN activation of ammonium sulfate and sodium chloride aerosol particles in theory and experiment. Atmos. Chem. Phys. 8, 1153–1179. https://doi.org/10.5194/acp-8-1153-2008.

Rose, D., Nowak, A., Achtert, P., Wiedensohler, A., Hu, M., Shao, M., Zhang, Y., Andreae, M.O., Pöschl, U., 2010. Cloud condensation nuclei in polluted air and biomass burning smoke near the mega-city Guangzhou, China – Part 1: size-resolved measurements and implications for the modeling of aerosol particle hygroscopicity and CCN activity. Atmos. Chem. Phys. 10, 3365–3383. https://doi.org/10.5194/acp-10-3365-2010.

Rosenørn, T., Kiss, G., Bilde, M., 2006. Cloud droplet activation of saccharides and levoglucosan particles. Atmos. Environ. 40, 1794–1802. https://doi.org/10.1016/j.atmosenv.2005.11.024.

Ruehl, C.R., Chuang, P.Y., Nenes, A., 2010. Aerosol hygroscopicity at high (99 to 100%) relative humidities. Atmos. Chem. Phys. 10, 1329–1344. https://doi.org/10.5194/acp-10-1329-2010.

Ruehl, C.R., Chuang, P.Y., Nenes, A., 2008. How quickly do cloud droplets form on atmospheric particles? Atmos. Chem. Phys. 8, 1043–1055. https://doi.org/10.5194/acp-8-1043-2008.

Ruehl, C.R., Davies, J.F., Wilson, K.R., 2016. An interfacial mechanism for cloud droplet formation on organic aerosols. Science (80-) 351, 1447–1450. https://doi.org/10.1126/science.aad4889.

Schmale, J., Henning, S., Henzing, B., Keskinen, H., Sellegri, K., Ovadnevaite, J., Bougiatioti, A., Kalivitis, N., Stavroulas, I., Jefferson, A., Park, M., Schlag, P., Kristensson, A., Iwamoto, Y., Pringle, K., Reddington, C., Aalto, P., Äijälä, M., Baltensperger, U., Bialek, J., Birmili, W., Bukowiecki, N., Ehn, M., Fjæraa, A.M., Fiebig, M., Frank, G., Fröhlich, R., Frumau, A., Furuya, M., Hammer, E., Heikkinen, L., Herrmann, E., Holzinger, R., Hyono, H., Kanakidou, M., Kiendler-Scharr, A., Kinouchi, K., Kos, G., Kulmala, M., Mihalopoulos, N., Motos, G., Nenes, A., O'Dowd, C., Paramonov, M., Petäjä, T., Picard, D., Poulain, L., Prévôt, A.S.H., Slowik, J., Sonntag, A., Swietlicki, E., Svenningsson, B., Tsurumaru, H., Wiedensohler, A., Wittbom, C., Ogren, J.A., Matsuki, A., Yum, S.S., Myhre, C.L., Carslaw, K., Stratmann, F., Gysel, M., 2017. Collocated observations of cloud condensation nuclei, particle size distributions, and chemical composition. Sci. Data 4, 170003. https://doi.org/10.1038/sdata.2017.3.

Seidl, W., 2000. Model for a surface film of fatty acids on rain water and aerosol particles. Atmos. Environ. 34, 4917–4932. https://doi.org/10.1016/S1352-2310(00)00198-9.

Seinfeld, J.H., Pandis, S.N., Noone, K., 1998. Atmospheric chemistry and physics: from air pollution to climate change. Phys. Today 51, 88–90. https://doi.org/10.1063/1.882420.

Shantz, N.C., Pierce, J.R., Chang, R.Y.-W., Vlasenko, A., Riipinen, I., Sjostedt, S., Slowik, J.G., Wiebe, A., Liggio, J., Abbatt, J.P.D., Leaitch, W.R., 2012. Cloud condensation nuclei droplet growth kinetics of ultrafine particles during anthropogenic nucleation events. Atmos. Environ. 47, 389–398. https://doi.org/10.1016/j.atmosenv.2011.10.049.

Sorjamaa, R., Svenningsson, B., Raatikainen, T., Henning, S., Bilde, M., Laaksonen, A., 2004. The role of surfactants in Köhler theory reconsidered. Atmos. Chem. Phys. 4, 2107–2117. https://doi.org/10.5194/acp-4-2107-2004.

Steiner, A.L., Brooks, S.D., Deng, C., Thornton, D.C.O., Pendleton, M.W., Bryant, V., 2015. Pollen as atmospheric cloud condensation nuclei. Geophys. Res. Lett. 42, 3596–3602. https://doi.org/10.1002/2015GL064060.

Stone, E.A., Mampage, C.B.A., Hughes, D.D., Jones, L.M., 2021. Airborne sub-pollen particles from rupturing giant ragweed pollen. Aerobiologia 37, 625–632. https://doi.org/10.1007/s10453-021-09702-x.

Tanarhte, M., Bacer, S., Burrows, S., Huffman, J., Pierce, K., Pozzer, A., Sarda-Estève, R., Savage, N., Lelieveld, J., 2018. Global modeling of primary biological particle concentrations with the EMAC chemistry-climate model. Atmos. Chem. Phys. Discuss. 1–33. https://doi.org/10.5194/acp-2018-361.

Tao, J., Kuang, Y., Luo, B., Liu, L., Xu, H., Ma, N., Liu, P., Xue, B., Zhai, M., Xu, Wanyun, Xu, Weiqi, Sun, Y., 2023. Kinetic limitations affect cloud condensation nuclei activity measurements under low supersaturation. Geophys. Res. Lett. 50, e2022GL101603 https://doi.org/10.1029/2022GL101603.

Taylor, P.E., Flagan, R.C., Miguel, A.G., Valenta, R., Glovsky, M.M., 2004. Birch pollen rupture and the release of aerosols of respirable allergens. Clin. Exp. allergy J. Br. Soc. Allergy Clin. Immunol. 34, 1591–1596. https://doi.org/10.1111/j.1365-2222.2004.02078.x.

Thalman, R., de Sá, S.S., Palm, B.B., Barbosa, H.M.J., Pöhlker, M.L., Alexander, M.L., Brito, J., Carbone, S., Castillo, P., Day, D.A., Kuang, C., Manzi, A., Ng, N.L., Sedlacek III, A.J., Souza, R., Springston, S., Watson, T., Pöhlker, C., Pöschl, U., Andreae, M.O., Artaxo, P., Jimenez, J.L., Martin, S.T., Wang, J., 2017. CCN activity and organic hygroscopicity of aerosols downwind of an urban region in central Amazonia: seasonal and diel variations and impact of anthropogenic emissions. Atmos. Chem. Phys. 17, 11779–11801. https://doi.org/10.5194/acp-17-11779-2017.

Titos, G., Jefferson, A., Sheridan, P.J., Andrews, E., Lyamani, H., Alados-Arboledas, L., Ogren, J.A., 2014. Aerosol light-scattering enhancement due to water uptake during the TCAP campaign. Atmos. Chem. Phys. 14, 7031–7043. https://doi.org/10.5194/acp-14-7031-2014.

Topping, D.O., McFiggans, G.B., Coe, H., 2005. A curved multi-component aerosol hygroscopicity model framework: Part 1 – inorganic compounds. Atmos. Chem. Phys. 5, 1205–1222. https://doi.org/10.5194/acp-5-1205-2005.

Trovato, M., Forlani, G., Signorelli, S., Funck, D., 2019. Proline Metabolism and its Functions in Development and Stress Tolerance, pp. 41–72. https://doi.org/10.1007/978-3-030-27423-8-2.

Varga, Z., Kiss, G., Hansson, H.-C., 2007. Modelling the cloud condensation nucleus activity of organic acids on the basis of surface tension and osmolality measurements. Atmos. Chem. Phys. 7, 4601–4611. https://doi.org/10.5194/acp-7-4601-2007.

Vilà, M., Vayreda, J., Comas, L., Ibáñez, J.J., Mata, T., Obón, B., 2007. Species richness and wood production: a positive association in Mediterranean forests. Ecol. Lett. 10, 241–250. https://doi.org/10.1111/j.1461-0248.2007.01016.x.

Wang, J., Shilling, J.E., Liu, J., Zelenyuk, A., Bell, D.M., Petters, M.D., Thalman, R., Mei, F., Zaveri, R.A., Zheng, G., 2019. Cloud droplet activation of secondary organic aerosol is mainly controlled by molecular weight, not water solubility. Atmos. Chem. Phys. 19, 941–954. https://doi.org/10.5194/acp-19-941-2019.

Yang, F., Xue, H., Deng, Z., Zhao, C., Zhang, Q., 2012. A closure study of cloud condensation nuclei in the North China Plain using droplet kinetic condensational growth model. Atmos. Chem. Phys. 12, 5399–5411. https://doi.org/10.5194/acp-12-5399-2012.

Zhang, Y., Steiner, A.L., 2022. Projected climate-driven changes in pollen emission season length and magnitude over the continental United States. Nat. Commun. 13, 1234. https://doi.org/10.1038/s41467-022-28764-0.

Zieger, P., Fierz-Schmidhauser, R., Weingartner, E., Baltensperger, U., 2013. Effects of relative humidity on aerosol light scattering: results from different European sites. Atmos. Chem. Phys. 13, 10609–10631. https://doi.org/10.5194/acp-13-10609-2013.